Table 1. Classification of CISs identified in *Runx1*$^{+/+}$ and *Runx1*$^{-/-}$ mice

Classification of CIS/chromosome number*	Gene†	*Runx1*$^{+/+}$, n = 52	*Runx1*$^{-/-}$, n = 63
Known CISs, n = 16			
5	*Gfi1/Evi5*‡	2	11 (1)§, (3)‖
15	*c-Myc*‡	3	11
17	*Ccnd3*‡	2	6
7	*RRas2*	4	5
10	*Ahi1/Myb*	7 (1)¶	3 (2)#
2	*Rasgrp1*	2	2
11	*Ikaros***	1	2
3	*Evi1*‡	0	5
6	*Ccnd2*‡	0	3
12	*N-myc*‡,**	0	3
17	*Pim1*	0	3
2	*Bcas1*	0	2
5	*Bcl7a*	0	2
5	*Mad1l1***	0	2
7	*Sema4b*	0	2
12	*Jundm2*	0	2
Novel CIS, n = 4			
X	*Slis6*	0	4
3	*Slis7*	0	3
5	*Slis8*	0	2
16	*Slis9*	0	2

CIS indicates common integration site; and RIS, retroviral integration site.

*The genomic positions of the RIS were determined according to BLAT search of the UCSC Genome Bioinformatics database.

†Candidate genes in the vicinity of the RIS are shown.

‡CISs that are particularly interesting and are discussed in the text.

§Number in parentheses indicates number of integrations inside *Gfi1*.

‖Number in parentheses indicates number of integrations inside *Evi5*.

¶Number in parentheses indicates number of integrations inside *Myb*.

#Number in parentheses indicates number of integrations inside *Ahi1*.

**Genes with all retroviral integrations inside the gene.

expressing both the T-cell and myeloid markers simultaneously (supplemental Figure 2A).

In *Runx1*$^{-/-}$ mice, 34 of 54 (63.6%) developed early-onset (≤ 24 weeks) leukemia/lymphoma, whereas only 19 of 52 (36.5%) *Runx1*$^{+/+}$ mice showed early onset of leukemia/lymphoma. Out of the early-onset cases, 51.4% of *Runx1*$^{-/-}$ cases and 15.8% of *Runx1*$^{+/+}$ cases showed leukemia with myeloid features that fell into groups 1 and 2. The remaining mice developed T-cell leukemia/lymphoma that fell into groups 3 and 4 (Figure 3C). This result indicates that *Runx1* knockout status drives myeloid features in leukemias despite the strong T-lymphoid tropism of MoMuLV virus. Some of the group 1 and 2 leukemias recapitulated human RUNX leukemias with accumulation of immature blasts (as seen in AML M0) or accumulation of myeloid cells with differentiation (as seen in AML M2; Figure 3D).

Stemness related genes are preferentially affected in *Runx1*$^{-/-}$ leukemias

There were 710 retroviral integration sites (RISs) found in 63 *Runx1*$^{-/-}$ mice and 52 *Runx1*$^{+/+}$ mice. These sequences were mapped to the mouse genome to identify the chromosomal location of the sequences and to identify candidate genes at the loci. Twenty loci were affected more than once by retroviral integrations in *Runx1*$^{-/-}$ or *Runx1*$^{+/+}$ mice and these are referred to as common integration sites (CISs; Table 1). The relative locations of these integration sites were compared with the tags from the publicly available Retroviral-Tagged Cancer Gene Database.[27] This comparison revealed that 16 CISs correspond to previously known loci where retroviral integration occurred more than once. The other 4 CISs were detected only by our study and have been designated as Slis (Singapore leukemia integration site) and classified as novel CISs (Table 1, supplemental Table 3).

Genes near CISs that are affected with high frequency in *Runx1*$^{-/-}$ mice, but affected with lower frequency in *Runx1*$^{+/+}$ mice, may be specifically involved in leukemogenesis of *Runx1*$^{-/-}$ mice. Notably, candidate leukemogenic genes near CISs in Runx1-deficient leukemias with myeloid features are more relevant to our study since these leukemias recapitulate human RUNX1-related leukemias. A comprehensive list of genes (near CISs or RISs) that may be involved in tumor progression of each leukemia sample with myeloid features is given in Table 2. Interestingly, 10 of 18 *Runx1*$^{-/-}$ mice that developed leukemia with myeloid features had integrations near stem cell–related genes such as *Gfi1/Evi5*, *Evi1*, and *Lmo2*. These CISs are rarely affected in T-cell leukemia/lymphoma and preferentially hit in leukemia with myeloid features (supplemental Table 4).

Integrations at the *Gfi1/Evi5* locus, the locus where these 2 genes are located in the same direction in no overlapping fashion, were found in 11 of 63 *Runx1*$^{-/-}$ mice analyzed and only in 2 of 52 *Runx1*$^{+/+}$ mice ($P < .05$, Fisher test). Seven of the 11 *Runx1*$^{-/-}$ leukemia cases with integrations at the *Gfi1/Evi5* locus belonged to groups 1 and 2 (n = 18), which showed early-onset leukemia with myeloid features (Table 2). Gfi1 is a well-known factor involved in stem cell maintenance,[28] while Evi5 was recently shown to be a cell-cycle regulator that prevents premature entry of cells into mitosis.[29] Expression levels of *Gfi1* and *Evi5* were examined by qRT-PCR on cDNA from 6 of the available leukemic samples with integrations at this locus and 3 control samples without integration at this locus (Figure 4A). *Evi5* overexpression was seen in all affected *Runx1*$^{-/-}$ cases with integration outside this gene, and became pronounced as the distance between the RIS and the *Evi5* gene decreased. This indicates specific, integration site–dependent activation of *Evi5* expression. *Gfi1* expression was not significantly affected by viral integrations in majority of the cases (Figure 4B). Thus, *Evi5* overexpression appears to play a more cooperative role with Runx1 deficiency in leukemogenesis. Out of the integrations that were present only in *Runx1*$^{-/-}$ mice and not in *Runx1*$^{+/+}$ mice, the most frequent were integrations at the *Evi1* locus seen in 5 *Runx1*$^{-/-}$ mice, 3 of which belonged to groups 1 and 2 (Table 2). Evi1 functions in self-renewal, maintenance, and proliferation of stem cells.[30,31] Integrations near *c-Myc*, *Cyclin D2*, and *Cyclin D3* genes were also more frequent in *Runx1*$^{-/-}$ mice. *c-Myc* is a well-known protooncogene that causes uncontrolled proliferation of cells when overexpressed. *Cyclin D2* and *D3* are G_1 cyclins and their dysregulation leads to abnormal cycling of cells (Table 2).

Overexpression of *EVI5* cooperates with *Runx1*$^{-/-}$ status in long-term maintenance of aberrant stem/progenitor cells in vitro

To examine the details of cooperation with *Runx1*$^{-/-}$ status, *Gfi1*, *Evi5*, and *Evi1* were chosen from the RIM screen due to high frequency of viral integrations near these genes in *Runx1*$^{-/-}$ leukemias compared with wild-type cases. We deduced that they are likely to prevent exhaustion of *Runx1*$^{-/-}$ stem cells due to their possible function in stem cell maintenance and thus contribute to development of Runx1-related leukemia.

To study the effect of overexpression of these candidate oncogenes in immature hematopoietic cells, the c-Kit$^+$ fraction of BM cells transfected with MIG vector carrying *GFI*, *EVI5*, or *EVI1*

Table 2. Cooperating genetic changes in leukemic mice belonging to groups 1 and 2

Group/tumor ID	Genotype	Stem cell*	Proliferation*	Tumor suppressor*	Novel	Others
Group 1: myeloid leukemia						
696	*Runx1*$^{-/-}$	*Gfi1/Evi5* (c)	*c-Myc* (c)			
807	*Runx1*$^{-/-}$		*Ncoa2*‡	*Ing4*		*Rbm34*
966	*Runx1*$^{-/-}$	*Evi1* (c)	*IL6st*			
714	*Runx1*$^{-/-}$	*Gfi1/Evi5* (c)	*Cyclin D3* (c), *Cyclin D2* (c)	*Dab2*‡		*Lfng, Swap70*
708	*Runx1*$^{-/-}$	*Evi1* (c)	*Pik3cd*	*Mapk9* (Jnk)	*Slis7* (c)	*Tmem23*‡
Group 2: biphenotypic leukemia						
691†	*Runx1*$^{-/-}$					
813	*Runx1*$^{-/-}$	*Gfi1/Evi5* (c)‡			*Slis6* (c)	*Arhgap25*
775	*Runx1*$^{-/-}$		*c-Myc* (c)			*Gimap7, Ak1*
770	*Runx1*$^{-/-}$		*Cyclin D3* (c), *Sema4d*	*Gadd45*	*Slis7* (c)	*Cspg4,* mSin3a
641	*Runx1*$^{-/-}$		*Cyclin D3* (c), *Cyclin D2* (c)	*Stag1*§	*Slis8* (c)	*Ang 2*
819	*Runx1*$^{-/-}$	*Gfi1/Evi5* (c)				*Stx4a, Negr1*
821	*Runx1*$^{-/-}$					
779	*Runx1*$^{-/-}$		*c-Myc* (c)	*Nkd1*	*Slis8* (c)	
982	*Runx1*$^{-/-}$	Gfi1/Evi5 (c)		*Stag1*§	*Slis6* (c)	*Limk2*
972	*Runx1*$^{-/-}$					*Ppfibp1*
969	*Runx1*$^{-/-}$	*Gfi1/Evi5* (c), *Evi1* (c)	*N-myc* (c)‡, *Cyclin D1* (c)	*Mad1l1*‡		*Rabggtb*
948	*Runx1*$^{-/-}$	*Gfi1/Evi5* (c)	*N-myc* (c)‡			*Stk16, Mdm4*
974	*Runx1*$^{-/-}$	*Lmo2*‖	*c-Myc* (c), *Cyclin D3* (c), *Lef1*			*Ldb1*
693	*Runx1*$^{+/+}$		*Tnfrsf191*	*Tspan32*		
690	*Runx1*$^{+/+}$	*Lmo2*‖		*Foxp1*		
663	*Runx1*$^{+/+}$	*Gfi1/Evi5* (c)	*Pip5k2a*‡			*Ugcg*
Unclassified‡						
2	*Runx1*$^{-/-}$	*Gfi1/Evi5* (c)	*N-myc* (c)‡, *Sept9, Pim2*			
4	*Runx1*$^{-/-}$	*Gfi1/Evi5* (c)‡, *Hes1*	*IL2*		*Slis6* (c)	*Birc4*
998	*Runx1*$^{-/-}$	*Gfi1/Evi5* (c)				
838	*Runx1*$^{-/-}$	*Gfi1/Evi5* (c)‡				

Table shows the genes near CISs or RISs that may have a role in oncogenesis based on their known or predicted function. (c) indicates CISs identified in this study. Leukemia cases in each group are arranged in ascending order of latency.

*Known or predicted function.

†RIS information is not available for this sample.

‡Genes with retroviral integrations inside the gene.

§Unclassified leukemia cases, which could belong to group 1 or 2; they showed early onset of disease and no enlargement of thymus/lymph node, and flow cytometric data are not available.

‖Gene near 2 RISs that cannot be classified as CISs based on definition.

was isolated by FACS and subjected to the experiments. LTC-IC assay was carried out after 30 days' culture of transfected *Runx1*$^{-/-}$ and *Runx1*$^{+/+}$ immature cells (GFP$^+$c-Kit$^+$) on OP9 stromal cells. The plating efficiency (colony number) of *Runx1*$^{-/-}$ cells with overexpression of *EVI5* gene was prominently high while that of mock-transfected *Runx1*$^{-/-}$ cells or *EVI5*-transfected *Runx1*$^{+/+}$ cells was lost, suggesting that cells overexpressing *EVI5* maintain a higher number of stem cells than other combinations (Figure 5A-B). When replated after 30 days, *Runx1*$^{-/-}$ cells carrying *EVI5* also showed a significantly high number of cobblestone area forming cells (CAFCs; Figure 5C). Furthermore, colony assay and CAFC assay after 30 more days of culture of replated cells (total 60 days after initial transfection) still showed a high number of colonies and CAFCs in *Runx1*$^{-/-}$ cells overexpressing *EVI5*. *GFI1*- and *EVI1*-transfected *Runx1*$^{+/+}$ or *Runx1*$^{-/-}$ cells did not show any colony or CAFCs after 30 days of LTC (Figure 5A,C).

Morphologic analyses of cells after 30 and 60 days of LTC revealed that *Runx1*$^{-/-}$ cells overexpressing *EVI5* have immature cell morphology characterized by nucleus with fine chromatin and basophilic cytoplasm. *Runx1*$^{-/-}$ cells transfected with mock vector and *Runx1*$^{+/+}$ cells overexpressing *EVI5* showed differentiated mast cell and macrophage morphology after 30 days of LTC (Figure 5D).

Taken together, the overexpression of *EVI5* strongly cooperates with *Runx1*$^{-/-}$ status in maintenance and proliferation of stem cells, and overexpression of *GFI1* or *EVI1* does not show significant cooperation in the OP9 culture. However, colony replating assay showed modest cooperation between *Runx1*$^{-/-}$ status and *EVI1* overexpression (supplemental Figure 3A).

Overexpression of *EVI5* and *EVI1* prevents exhaustion of *Runx1*$^{-/-}$ stem cells in vivo

To assess the in vivo effect, *EVI5* transfected *Runx1*$^{-/-}$ or *Runx1*$^{+/+}$ cells were transplanted into sublethally irradiated (6 Gy) recipient mice. Recipients of *Runx1*$^{+/+}$ cells transfected with *EVI5* showed stable GFP chimerism throughout, from 6 weeks to 30 weeks after transplantation, with an average of 20% to 25%. However, the GFP chimerism of mice that underwent transplantation with *Runx1*$^{-/-}$ cells overexpressing *EVI5* increased progressively, with a mean value of 25% at 6 weeks and 50% at 30 weeks

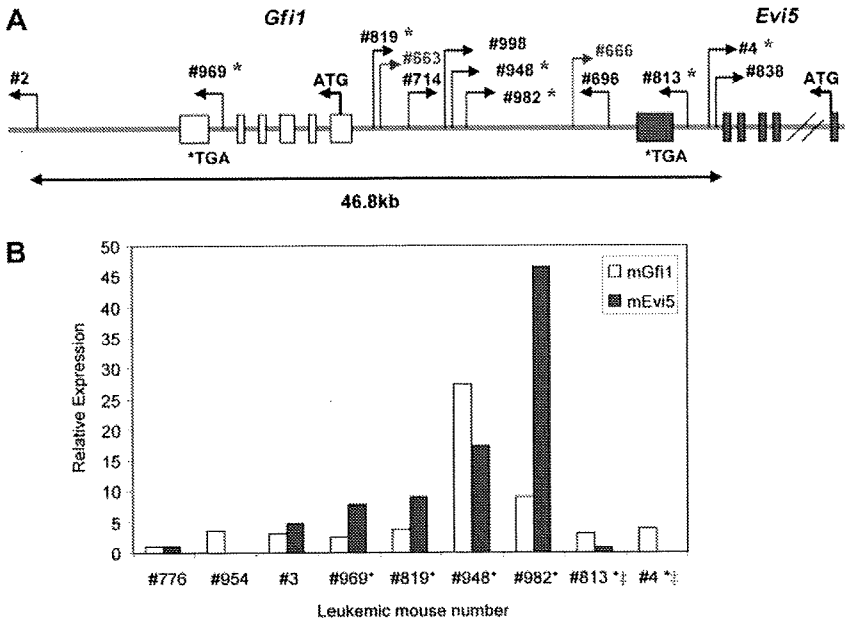

Figure 4. Frequent integrations at *Gfi1/Evi5* locus in *Runx1*$^{-/-}$ leukemias lead to overexpression of *Evi5*. (A) Schematic diagram of retroviral integration sites at *Gfi1/Evi5* locus in 2 *Runx1*$^{+/+}$ and 11 *Runx1*$^{-/-}$ leukemias. Numbers are unique to each leukemic mouse. Thin bent arrows represent the retrovirus integration site and its direction of integration. The 2 genes *Gfi* (light gray) and *Evi5* (dark gray) span from their initiation codons (ATG) to stop codons (TGA) with boxes representing exons. *Leukemia cases in which expression of *Gfi1* and *Evi5* was checked using qRT-PCR. (B) qRT-PCR analysis of *Gfi1* and *Evi5* expression in leukemic cells harboring integrations at *Gfi1/Evi5* locus (*), integrations within the *Evi5* gene (‡), and 3 control samples without integrations at this locus. Data are represented as fold change relative to control sample no. 776.

(Figure 5E). This is in contrast to the results seen after transplantation of mock vector–transfected *Runx1*$^{-/-}$ cells described earlier where the contribution of *Runx1*$^{-/-}$ cells to PB of recipient mice decreased progressively (Figure 1C). Thus, *EVI5* cooperates with *Runx1*$^{-/-}$ status in vivo also by preventing stem cell exhaustion and maintaining an increased number of *Runx1*-deficient stem cells. A secondary transplantation experiment was repeated to examine whether *EVI5* overexpression in *Runx1*$^{-/-}$ cells could rescue the defects in long-term repopulating abilities of *Runx1*$^{-/-}$ stem cells. Contrary to the previous results where 60% of the secondary recipients of *Runx1*$^{-/-}$ cells died within 3 months, all the secondary recipients of *Runx1*$^{-/-}$ cells overexpressing *EVI5* were alive (Figure 5F). We conclude that *EVI5* overexpression in *Runx1*$^{-/-}$ cells can prevent stem cell exhaustion of these cells and render them capable of reconstituting hematopoiesis in the secondary recipients.

As colony replating assay showed mild cooperation between *EVI1* overexpression and *Runx1*$^{-/-}$ status (supplemental Figure 3A), BMT was carried out for *EVI1* overexpressing cells as well. Recipients of *Runx1*$^{+/+}$ and *Runx1*$^{-/-}$ cells transfected with *EVI1* showed stable GFP chimerism throughout, from 6 weeks to 30 weeks after transplantation, with no significant increase or decrease in GFP chimerism (supplemental Figure 3B). Thus, *EVI1* overexpression also seems to rescue *Runx1*$^{-/-}$ stem cell exhaustion in vivo.

EVI5 is overexpressed in 44% of human patients with AML M2 RUNX leukemia

To evaluate whether *EVI5* overexpression synergizes with loss-of-function of RUNX1 in human patients with RUNX1-related leukemia, we carried out qRT-PCR on cDNA from patient samples with AML M2 carrying *RUNX1-ETO* fusion gene or AML M4Eo carrying *CBFB-MYH11* fusion gene. These fusion genes are more commonly found *RUNX1* alterations and they lead to loss-of-function of RUNX1. Expression of *EVI5* in other AML and CML samples without known RUNX1 alterations was also analyzed. cDNA from BM of 3 patients who had undergone complete remission was used as control. Indeed, very significant overexpression of *EVI5* was seen in 4 of 9 (44%) AML M2 patients examined. AML M4Eo patients also showed 2- to 3-fold overexpression as compared with control samples and AML samples without RUNX1 alteration (Figure 6). Thus, *EVI5* overexpression and concomitant loss-of-function of RUNX1 are often observed in human RUNX1-related leukemia cases, especially in AML M2 carrying *RUNX1-ETO* fusion gene, suggesting that EVI5 is likely to prevent stem cell exhaustion in human RUNX1-related leukemias.

Runx1$^{-/-}$ stem cell exhaustion may be due to defective interaction with the niche

Interaction of stem cells with the stem cell niche is important for maintaining the integrity and self-renewal properties of stem cells.[32,33] Analysis of a panel of niche-related factors in immature cell fraction (c-Kit^{+}GFP^{+}) of MIG vector–transfected *Runx1*$^{+/+}$ and *Runx1*$^{-/-}$ BM cells, revealed that one of the most important molecules for interaction with the stem cell niche, Cxcr4, was down-regulated in *Runx1*$^{-/-}$ cells. However, normal level of Cxcr4 expression was restored after overexpression of *EVI5* in *Runx1*$^{-/-}$ cells (supplemental Figure 4A). The down-regulation of Cxcr4 expression in the *Runx1*$^{-/-}$ stem/progenitor (KSL) cell fraction was further confirmed by flow cytometry ($P < .001$) and qRT-PCR ($P < .005$) (Figure 7A). Cxcr4 expression was also down-regulated in wild-type immature (c-Kit^{+}) BM cells transfected with the dominant-negative chimeric gene *RUNX1-ETO*, indicating that niche interaction may be altered in human RUNX1-related leukemic cases (Figure 7B). The qRT-PCR result indicates transcriptional regulation of *Cxcr4* expression by Runx1. Indeed, 2 RUNX binding sites are present in the *CXCR4* promoter region, and luciferase assay using the *CXCR4* promoter region showed that RUNX1 transactivates *CXCR4* more than 20-fold, in a DNA binding–dependent manner (Figure 7C). Along with Cxcr4, another niche interacting factor, CD49b, which is an α2 integrin, was also down-regulated in immature *Runx1*$^{-/-}$ cells and its expression restored to normal after overexpression of *EVI5* in these cells (supplemental Figure 4A).

We carried out a homing assay to evaluate whether *Runx1*$^{-/-}$ BM cells are compromised in homing and niche interaction. Five million BM cells from *Runx1*$^{+/+}$ and *Runx1*$^{-/-}$ mice were labeled with 100% efficiency by CFSE, and transplanted into recipient mice. Analysis of recipient BM 16 hours after transplantation revealed that *Runx1*$^{-/-}$ cells traffic to the BM with significantly reduced efficiency (Figure 7D, supplemental Figure 4B). Thus,

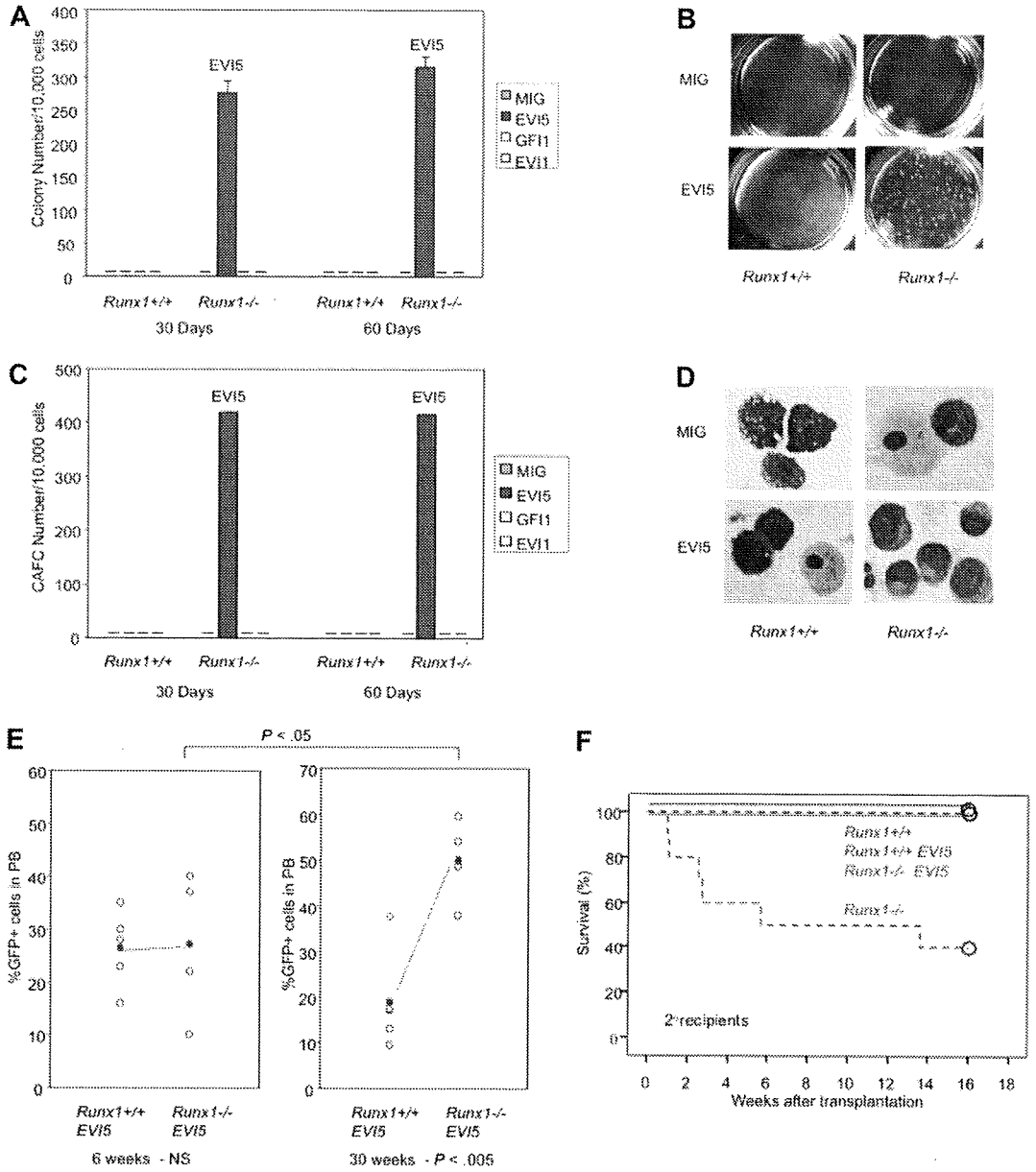

Figure 5. EVI5 overexpression and *Runx1*$^{-/-}$ status synergize in long-term maintenance of stem cells in vitro and in vivo. Graphic representation of (A) colony assay and (C) CAFC assay of immature cells from *Runx1*$^{+/+}$ and *Runx1*$^{-/-}$ BM cells transfected with mock MIG vector, *EVI5*, *GFI1*, or *EVI1*, after 30 and 60 days of long-term culture. Pictures of (B) colonies and (D) morphology of cells after 30 days of long-term culture. (E) GFP chimerism in recipients of *Runx1*$^{+/+}$ (n = 5) and *Runx1*$^{-/-}$ (n = 4) BM cells transfected with *EVI5*, 6 and 30 weeks after transplantation. Each open circle represents data from an individual mouse and the closed red circle is the average of a cohort. Statistical difference using unpaired Student *t* test is given at the bottom and on top. NS indicates not significant. (F) Kaplan-Meier survival curves of secondary recipients of *Runx1*$^{+/+}$ (blue; n = 4) and *Runx1*$^{-/-}$ (red; n = 4) BM cells transfected with mock MIG vector (dashed line) or MIG vector carrying *EVI5* (solid line). Circles represent end point of analysis.

altered ability to home and attach to the stem cell niche in the BM may be one of the reasons for *Runx1*$^{-/-}$ stem cell exhaustion.

To assess whether defects in niche interaction of Runx1-deficient HSCs lead to mobilization of stem/progenitor cells to the PB and spleen, we carried out colony assay of PB and flow cytometry analysis of spleen cells from *Runx1*$^{-/-}$ and *Runx1*$^{+/+}$ mice. PB (20 μL) from each *Runx1*$^{-/-}$ mouse formed an average of 35 colonies while PB from *Runx1*$^{+/+}$ mice did not form any colonies (Figure 7E). Similarly, a significantly higher number of stem/progenitor cells was present in the spleen of *Runx1*$^{-/-}$ mice (Figure 7F). These results indicate that Runx1 deficiency leads to dramatic egress of HSCs from the BM into the PB and spleen.

We also carried out a BrdU incorporation assay to analyze whether there is increased proliferation of HSC compartment of *Runx1*$^{-/-}$ mice due to their defective niche interaction and increased cell-cycle entry. As shown in Figure 7G, proliferation of stem/progenitor cells (KSL fraction) was strongly induced in *Runx1*$^{-/-}$ mice, resulting in approximately 7-fold more BrdU^{+} stem/progenitor cells in *Runx1*$^{-/-}$ mice ($P < .05$). Taken together, all the above results suggest that the interaction between *Runx1*$^{-/-}$ HSC and its niche may be perturbed, probably due to reduced expression of Cxcr4, resulting in the release of stem cells from the niche, leading to initial expansion and subsequent exhaustion of HSCs (supplemental Figure 5B).

Finally, expression of several genes involved in stem cell function and apoptosis were checked in immature (c-Kit^{+}) cell fraction of mock- or *EVI5*-transfected (GFP^{+}) BM cells from *Runx1*$^{+/+}$ and *Runx1*$^{-/-}$ mice, by qRT-PCR. Among the candidate genes tested, *Bmi-1*, important for self-renewal of normal and cancer stem cells,[34] and the antiapoptotic gene, *Bcl2*, which is negatively regulated by Runx family,[35,36] were overexpressed in

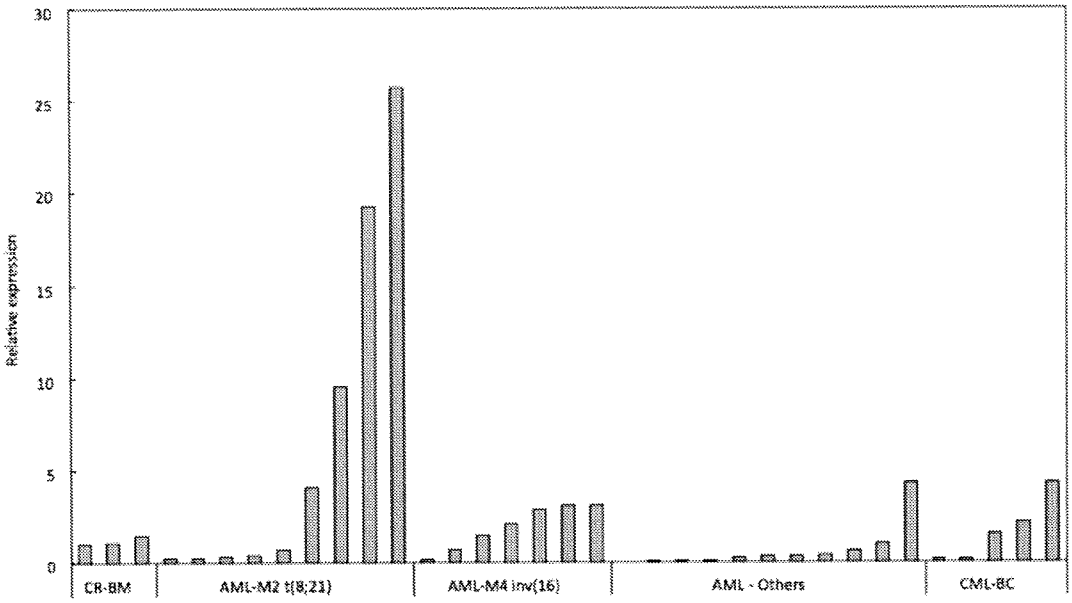

Figure 6. EVI5 is overexpressed in human RUNX leukemia. qRT-PCR analysis of *EVI5* expression in human RUNX1-related leukemia samples: AML M2 with t(8;21) resulting in RUNX1-ETO fusion protein, AML M4 with inv(16) resulting in PEBP2β-SMMHC fusion protein, other AML cases without *RUNX1* alteration and CML cases with blast crisis (CML-BC). Data are represented as fold change relative to BM samples undergoing complete remission (CR-BM).

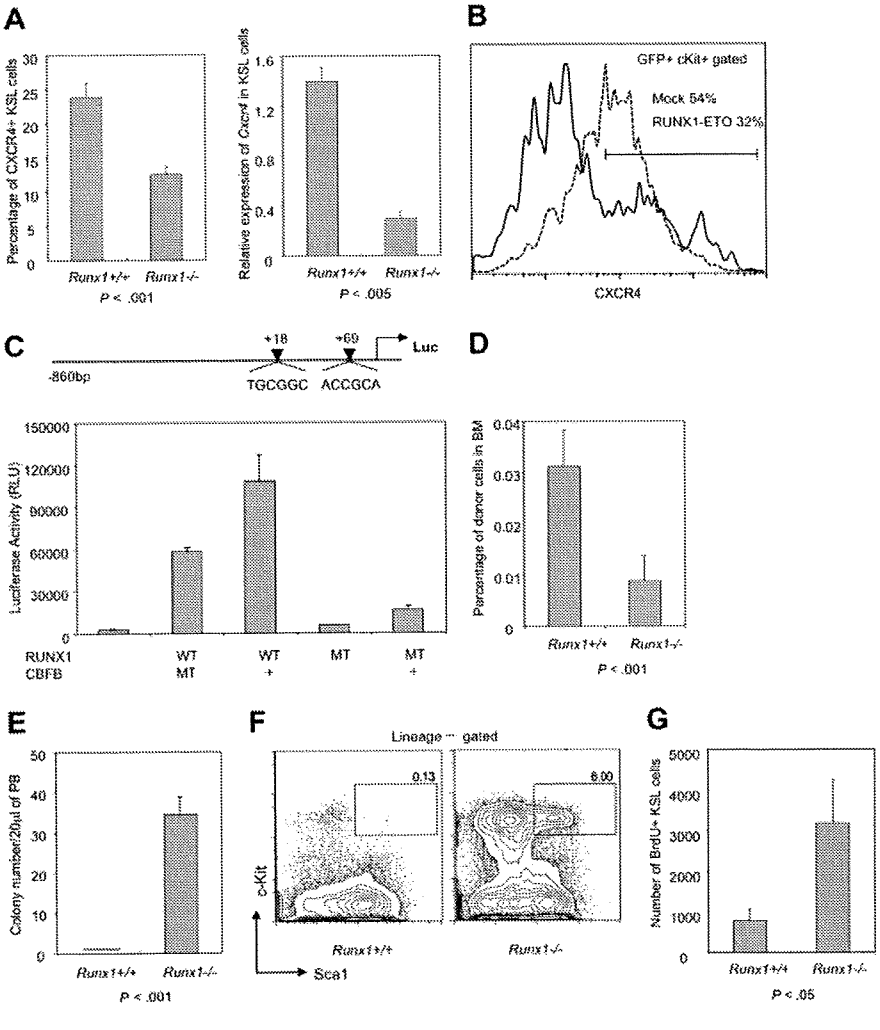

Figure 7. Decreased expression of niche factor, Cxcr4, and impaired homing may be responsible for *Runx1*$^{-/-}$ stem cell exhaustion. (A) Left panel: flow cytometric analysis of Cxcr4 expression on KSL cells from *Runx1*$^{+/+}$ (n = 4) and *Runx1*$^{-/-}$ (n = 3) mice. Right panel: qRT-PCR analysis of expression of *Cxcr4* in KSL fraction of *Runx1*$^{+/+}$ and *Runx1*$^{-/-}$ BM cells. Statistical difference using unpaired Student *t* test is given at the bottom. (B) Expression of Cxcr4 in c-Kit^{+}GFP^{+} cells from wild-type BM cells transfected with mock MIG vector (dashed line) or *RUNX1-ETO* (solid line). One representative result of 2 experiments is shown. (C) Structure of the CXCR4 promoter luciferase reporter construct. The 2 arrowheads represent the positions of 2 consensus Runx1 binding sites on the human *CXCR4* promoter. Graph represents the result of luciferase assay, showing transcriptional activity of wild-type RUNX1 (WT) or its mutant form R174Q (MT) with (+) or without CBFB, on *CXCR4* promoter. (D) Graph showing percentage of CFSE-stained *Runx1*$^{+/+}$ or *Runx1*$^{-/-}$ BM cells found in the recipient BM (n = 4 and 6, respectively), 16 hours after transplantation. Statistical difference using unpaired Student *t* test is given at the bottom. (E) Graphic representation of colony assay of 20 µL of PB from *Runx1*$^{+/+}$ (n = 4) and *Runx1*$^{-/-}$ (n = 4) mice. (F) FACS analysis of spleen KSL fraction in *Runx1*$^{+/+}$ and *Runx1*$^{-/-}$ mice. One representative flow cytometry profile from 2 experiments is shown. (G) Graph showing absolute number of BrdU^{+} KSL cells per 1 million BM cells analyzed from *Runx1*$^{-/-}$ (n = 3) and *Runx1*$^{+/+}$ mice (n = 3). Statistical difference using unpaired Student *t* test is given at the bottom.

Runx1$^{-/-}$ cells,[18] and the expression of these genes was further enhanced by overexpression of *EVI5* (data not shown).

Discussion

Loss-of-function of RUNX1 is frequently observed in human leukemia, implying that RUNX1 deficiency may predispose cells to leukemia development. Consistently, our previous study revealed that there is an expansion of the HSC/progenitor compartment in *Runx1*$^{-/-}$ mice, accompanied by resistance to cell death, senescence, and differentiation, characteristic of a leukemia-susceptible status.[18] Three other groups, who generated conditional *Runx1* knockout mice independently, also reported the expansion of the HSC/progenitor population.[15-17,37] However, there is no spontaneous leukemia development in the Runx1-deficient mice. In this report, we show that the reason for this paradox may be exhaustion of Runx1-deficient HSCs over time. We provided strong evidence for exhaustion of *Runx1*$^{-/-}$ stem cells using limiting dilution and secondary transplantation experiments. A similar conclusion was reported by others using competitive transplantation experiment.[16] Ichikawa et al also suggested that there appears to be a distinct difference in HSC numbers soon after deletion of *Runx1* alleles (4 to 9 weeks) and over long periods of time, although they described only the initial phase expansion.[37]

In order to understand the mechanism of *Runx1*$^{-/-}$ stem cell exhaustion, we explored cell intrinsic changes and alterations in stem cell niche interaction. Immature *Runx1*$^{-/-}$ cells expressed higher levels of *Bmi1* and *Bcl2*,[18] and they maintained their inherent proliferative ability at 40 weeks of age and even 2 years after transplantation (Figure 2B,C). These results suggest a cell-intrinsic bias toward survival rather than exhaustion of *Runx1*$^{-/-}$ cells. On the other hand, niche interaction, which is essential for maintaining the functional integrity and quiescence of HSCs, was impaired in immature *Runx1*$^{-/-}$ cells as evidenced by reduced expression of Cxcr4 in the KSL fraction, defective homing, and mobilization of HSCs from BM into PB and spleen. Conditional *Cxcr4* knockout mice show a very similar egress of HSCs from BM to PB and spleen,[38] supporting the notion that Cxcr4 could be the downstream factor that affects the niche interaction of Runx1-deficient cells. Quiescent LT-HSCs are found attached to osteoblasts in the endosteal niche of the trabecular bone. Under the steady-state condition, these HSCs are forced to leave their original niche and migrate to another niche due to continuous bone turnover. When there are coexisting wild-type HSCs in the cell milieu, HSCs that lack Runx1 could be outcompeted in establishing adequate interaction with another niche, leading to their slow exhaustion (supplemental Figure 5C). Thus, problems in niche interaction would be a critical issue in leukemia development, particularly at the initial step, and a leukemia initiating clone, or preleukemic stem cells, with *Runx1* alteration have to overcome this selective disadvantage for leukemia progression.

RIM to identify cooperating genetic alterations revealed that *Runx1*$^{-/-}$ mice injected with retrovirus showed shorter latency of leukemia development, thus confirming the leukemic predisposition of *Runx1*$^{-/-}$ status. There was a high frequency of stem cell–related genes affected in *Runx1*$^{-/-}$ mice and *EVI5* overexpression showed the most significant effect in rescuing stem cell exhaustion, followed by *EVI1* overexpression. Our results show that *EVI5* may rescue *Runx1*$^{-/-}$ stem cell exhaustion by restoring expression of Cxcr4 and CD49b (supplemental Figure 4A), which enables HSCs to home back and establish adequate interaction with the niche. It is well known that factors such as CXCR4 and CD44, which mediate homing and interaction with the stem cell niche, are often up-regulated in leukemia and are essential for maintenance of leukemic stem cells.[39-41] Thus, the ability of EVI5 to restore Runx1-deficient HSC interaction with its niche, together with other intrinsic factors, may be an important mechanism to rescue stem cell exhaustion, maintain leukemia-initiating stem cells, and promote leukemogenesis. It is not known how EVI5 mediates this effect. The role of EVI5 in the cell cycle may result in the indirect effects seen in HSC/progenitors since cell-cycle regulation is tightly linked to stem cell maintenance. Alternatively, EVI5 contains a conserved GAP domain, which has been shown to be important for actin cytoskeleton reorganization. Hematopoietic stem/progenitor cells from knockout mice of *Cdc42GAP*, one of the GAP domain family genes, showed impaired cortical F-actin assembly, deficiency in adhesion and migration, and defective homing and engraftment in the stem cell niche, leading to decline in stem cells.[42] EVI5 might play a similar role as Cdc42GAP and mediate homing and engraftment of Runx1-deficient HSCs through its GAP domain.

The recipient mice that underwent transplantation with *Runx1*$^{-/-}$ cells overexpressing *EVI5* or *EVI1* did not develop leukemia even 1 year after BMT, although the stem cell exhaustion was definitely rescued (Figure 5E-F, supplemental Figure 3B). Further genetic changes, such as strong mitogenic stimuli, are considered to be required for overt leukemia. Indeed, overexpression of oncogenes such as *c-Myc*, *N-Myc*, or *D-type cyclins* that promote cell proliferation was concurrently seen in 5 of 8 *Runx1*$^{-/-}$ leukemia cases showing *Evi5* overexpression in the RIM study (Table 2). In human RUNX1-related leukemia, similar mitogenic events such as mutations in receptor tyrosine kinases including *c-KIT* and *RAS* have been previously reported.[4,18] In fact, of the 4 human AML M2 cases carrying *RUNX1-ETO* which showed overexpression of *EVI5*, 3 cases had concurrent activating mutations in *c-KIT* or *FLT3*. Thus, these genetic alterations overlap with each other and act as second and third hits in RUNX1-related leukemia. Interestingly, mitogenic stimuli such as oncogenic Ras are shown to induce apoptosis, senescence, and differentiation, all of which function as negative factors for oncogenesis, and are considered as a vital cellular fail-safe mechanism. However, these detrimental effects due to oncogene stimulation are attenuated by Runx1-deficient status in the development of leukemia.[18] Similarly, negative effect of Runx1 deficiency, stem cell exhaustion, is in turn rescued by overexpresssion of *Evi5* and *Evi1*.

Considering the genes that are altered with high frequency in Runx1-related leukemias and the known properties and functions of these genes, we propose the following mechanism of Runx1-related leukemogenesis. Loss-of-function of Runx1 results in increase of stem/progenitor cell fraction and therefore serves as the target cell pool for leukemia. However, maintenance of *Runx1*$^{-/-}$ stem cells is compromised, probably due to the defect in interaction between HSC and niche, resulting in stem cell exhaustion. Overexpression of stem cell–related gene like *Evi5* rescues exhaustion of Runx1-deficient stem cells and maintains a significantly expanded pool of the aberrant cells with enhanced stem cell properties. Mitogenic stimuli such as activation of *c-Myc*, *N-myc*, *D-type cyclins*, *Ras*, or *c-Kit* result in overt proliferation of Runx1-deficient cells due to attenuated cellular fail-safe mechanism, thus providing the necessary stimulus for Runx1-deficient cells to develop full-blown leukemia. Such cooperative mechanism may be generally seen in cancer development whereby negative aspects caused by certain oncogenic hits are overcome by the others. Elucidation of these combinatorial mechanisms would provide profound insights into the understanding of oncogenesis and may provide a novel direction for therapeutic applications.

Acknowledgments

We thank M. Yanagida, L. Motoda, E. L. Ng, S. S. Nah, L. Q. Chen, and Q. R. Gwee for technical assistance and scientific discussions; N. Copeland and N. Jenkins for the MoMuLV retrovirus; M. Sugai for the MIG retroviral vector; G. P. Nolan for the Phoenix-Eco cell line; K. Morishita for human EVI1 cDNA; K. Rajewsky for Mx-Cre Tg mice; W. Krek for *CXCR4* promoter luciferase constructs; and members of the Biological Resource Center, Biopolis, for mouse husbandry.

This work was supported by A*STAR (Agency of Science, Technology and Research), Singapore National Research Foundation, and the Ministry of Education under the Research Center of Excellence Program.

Authorship

Contribution: B.J. and M.O. designed and performed experiments, analyzed data, and wrote the manuscript; N.Y. and C.Q.W. performed experiments; I.T. and D.R.L. provided the conditional *Runx1* knockout mice; N.A. provided the patient leukemic samples; and Y.I. analyzed data and contributed to writing the manuscript.

Conflict-of-interest disclosure: The authors declare no competing financial interests.

Correspondence: Motomi Osato or Yoshiaki Ito, Institute of Molecular and Cell Biology, 61 Biopolis Dr, Singapore 138673; e-mail: motomi@imcb.a-star.edu.sg or itoy@imcb.a-star.edu.sg.

References

1. Ito Y. RUNX genes in development and cancer: regulation of viral gene expression and the discovery of RUNX family genes. *Adv Cancer Res.* 2008;99:33-76.
2. Okuda T, van DJ, Hiebert SW, Grosveld G, Downing JR. AML1, the target of multiple chromosomal translocations in human leukemia, is essential for normal fetal liver hematopoiesis. *Cell.* 1996;84(2):321-330.
3. Wang Q, Stacy T, Binder M, et al. Disruption of the Cbfa2 gene causes necrosis and hemorrhaging in the central nervous system and blocks definitive hematopoiesis. *Proc Natl Acad Sci U S A.* 1996;93(8):3444-3449.
4. Speck NA, Gilliland DG. Core-binding factors in haematopoiesis and leukaemia. *Nat Rev Cancer.* 2002;2(7):502-513.
5. Castilla LH, Wijmenga C, Wang Q, et al. Failure of embryonic hematopoiesis and lethal hemorrhages in mouse embryos heterozygous for a knocked-in leukemia gene CBFB-MYH11. *Cell.* 1996;87(4):687-696.
6. Yergeau DA, Hetherington CJ, Wang Q, et al. Embryonic lethality and impairment of haematopoiesis in mice heterozygous for an AML1-ETO fusion gene. *Nat Genet.* 1997;15(3):303-306.
7. Song WJ, Sullivan MG, Legare RD, et al. Haploinsufficiency of CBFA2 causes familial thrombocytopenia with propensity to develop acute myelogenous leukaemia. *Nat Genet.* 1999;23(2):166-175.
8. Osato M, Asou N, Abdalla E, et al. Biallelic and heterozygous point mutations in the runt domain of the AML1/PEBP2alphaB gene associated with myeloblastic leukemias. *Blood.* 1999;93(6):1817-1824.
9. Osato M. Point mutations in the RUNX1/AML1 gene: another actor in RUNX leukemia. *Oncogene.* 2004;23(24):4284-4296.
10. Preudhomme C, Renneville A, Bourdon V, et al. High frequency of RUNX1 bi-allelic alteration in acute myeloid leukemia (AML) secondary to familial platelet disorder (FPD). *Blood.* 2009; 113(22):5583-5587.
11. Okuda T, Cai Z, Yang S, et al. Expression of a knocked-in AML1-ETO leukemia gene inhibits the establishment of normal definitive hematopoiesis and directly generates dysplastic hematopoietic progenitors. *Blood.* 1998;91(9):3134-3143.
12. Castilla LH, Garrett L, Adya N, et al. The fusion gene Cbfb-MYH11 blocks myeloid differentiation and predisposes mice to acute myelomonocytic leukaemia. *Nat Genet.* 1999;23(2):144-146.
13. Rhoades KL, Hetherington CJ, Harakawa N, et al. Analysis of the role of AML1-ETO in leukemogenesis, using an inducible transgenic mouse model. *Blood.* 2000;96(6):2108-2115.
14. Yuan Y, Zhou L, Miyamoto T, et al. AML1-ETO expression is directly involved in the development of acute myeloid leukemia in the presence of additional mutations. *Proc Natl Acad Sci U S A.* 2001;98(18):10398-10403.
15. Ichikawa M, Asai T, Saito T, et al. AML-1 is required for megakaryocytic maturation and lymphocytic differentiation, but not for maintenance of hematopoietic stem cells in adult hematopoiesis. *Nat Med.* 2004;10(3):299-304.
16. Growney JD, Shigematsu H, Li Z, et al. Loss of Runx1 perturbs adult hematopoiesis and is associated with a myeloproliferative phenotype. *Blood.* 2005;106(2):494-504.
17. Putz G, Rosner A, Nuesslein I, Schmitz N, Buchholz F. AML1 deletion in adult mice causes splenomegaly and lymphomas. *Oncogene.* 2006; 25(6):929-939.
18. Motoda L, Osato M, Yamashita N, et al. Runx1 protects hematopoietic stem/progenitor cells from oncogenic insult. *Stem Cells.* 2007;25(12):2976-2986.
19. Jonkers J, Berns A. Retroviral insertional mutagenesis as a strategy to identify cancer genes. *Biochim Biophys Acta.* 1996;1287(1):29-57.
20. van Lohuizen M, Verbeek S, Scheijen B, et al. Identification of cooperating oncogenes in E mu-myc transgenic mice by provirus tagging. *Cell.* 1991;65(5):737-752.
21. Nakamura T. Retroviral insertional mutagenesis identifies oncogene cooperation. *Cancer Sci.* 2005;96(1):7-12.
22. Yamashita N, Osato M, Huang L, et al. Haploinsufficiency of Runx1/AML1 promotes myeloid features and leukaemogenesis in BXH2 mice. *Br J Haematol.* 2005;131(4):495-507.
23. Yanagida M, Osato M, Yamashita N, et al. Increased dosage of Runx1/AML1 acts as a positive modulator of myeloid leukemogenesis in BXH2 mice. *Oncogene.* 2005;24(28):4477-4485.
24. Goemans BF, Zwaan CM, Miller M, et al. Mutations in KIT and RAS are frequent events in pediatric core-binding factor acute myeloid leukemia. *Leukemia.* 2005;19(9):1536-1542.
25. Taniuchi I, Osato M, Egawa T, et al. Differential requirements for Runx proteins in CD4 repression and epigenetic silencing during T lymphocyte development. *Cell.* 2002;111(5):621-633.
26. Kuhn R, Schwenk F, Aguet M, Rajewsky K. Inducible gene targeting in mice. *Science.* 1995; 269(5229):1427-1429.
27. Akagi K, Suzuki T, Stephens RM, Jenkins NA, Copeland NG. RTCGD: retroviral tagged cancer gene database. *Nucleic Acids Res.* 2004;32:D523-D527.
28. Hock H, Hamblen MJ, Rooke HM, et al. Gfi-1 restricts proliferation and preserves functional integrity of haematopoietic stem cells. *Nature.* 2004;431(7011):1002-1007.
29. Eldridge AG, Loktev AV, Hansen DV, et al. The evi5 oncogene regulates cyclin accumulation by stabilizing the anaphase-promoting complex inhibitor emi1. *Cell.* 2006;124(2):367-380.
30. Du Y, Spence SE, Jenkins NA, Copeland NG. Cooperating cancer-gene identification through oncogenic-retrovirus-induced insertional mutagenesis. *Blood.* 2005;106(7):2498-2505.
31. Yuasa H, Oike Y, Iwama A, et al. Oncogenic transcription factor Evi1 regulates hematopoietic stem cell proliferation through GATA-2 expression. *EMBO J.* 2005;24(11):1976-1987.
32. Moore KA, Lemischka IR. Stem cells and their niches. *Science.* 2006;311(5769):1880-1885.
33. Wilson A, Trumpp A. Bone-marrow haematopoietic-stem-cell niches. *Nat Rev Immunol.* 2006;6(2):93-106.
34. Iwama A, Oguro H, Negishi M, et al. Enhanced self-renewal of hematopoietic stem cells mediated by the polycomb gene product Bmi-1. *Immunity.* 2004;21(6):843-851.
35. Klampfer L, Zhang J, Zelenetz AO, Uchida H, Nimer SD. The AML1/ETO fusion protein activates transcription of BCL-2. *Proc Natl Acad Sci U S A.* 1996;93(24):14059-14064.
36. Frank RC, Sun X, Berguido FJ, Jakubowiak A, Nimer SD. The t(8;21) fusion protein, AML1/ETO, transforms NIH3T3 cells and activates AP-1. *Oncogene.* 1999;18(9):1701-1710.
37. Ichikawa M, Goyama S, Asai T, et al. AML1/Runx1 negatively regulates quiescent hematopoietic stem cells in adult hematopoiesis. *J Immunol.* 2008;180(7):4402-4408.
38. Sugiyama T, Kohara H, Noda M, Nagasawa T. Maintenance of the hematopoietic stem cell pool by CXCL12-CXCR4 chemokine signaling in bone marrow stromal cell niches. *Immunity.* 2006;25(6):977-988.
39. Krause DS, Lazarides K, von Andrian UH, Van Etten RA. Requirement for CD44 in homing and engraftment of BCR-ABL-expressing leukemic stem cells. *Nat Med.* 2006;12(10):1175-1180.
40. Jin L, Hope KJ, Zhai Q, Smadja-Joffe F, Dick JE. Targeting of CD44 eradicates human acute myeloid leukemic stem cells. *Nat Med.* 2006;12(10):1167-1174.
41. Tavor S, Petit I, Porozov S, et al. CXCR4 regulates migration and development of human acute myelogenous leukemia stem cells in transplanted NOD/SCID mice. *Cancer Res.* 2004;64(8):2817-2824.
42. Wang L, Yang L, Filippi MD, Williams DA, Zheng Y. Genetic deletion of Cdc42GAP reveals a role of Cdc42 in erythropoiesis and hematopoietic stem/progenitor cell survival, adhesion, and engraftment. *Blood.* 2006;107(1):98-105.

Bareford D, et al. Hydroxyurea compared with anagrelide in high-risk essential thrombocythemia. N Engl J Med 2005;353:33-45.
12. Thiele J, Kvasnicka HM. Myelofibrosis in chronic myeloproliferative disorders - dynamics and clinical impact. Histol Histopathol 2006;21:1367-78.

Myelofibrotic transformation in essential thrombocythemia. Author reply

We thank Juergen Thiele and Hans Kvasnicka for commenting on our recently published paper including 605 patients with essential thrombocythemia (ET).[1] We provided evidence that progression to myelofibrosis (post-ET MF) has a prevalence of 2.8% (10-year risk of 3.9%), and that progression to acute leukemia (AL) has a prevalence of 2.3% (10-year risk of 2.6%). The first question of Thiele and Kvasnicka concerns the evolution of ET in post-ET MF and AL. They asked that the prevalence of post-ET MF and AL in patients diagnosed according to the PVSG criteria[2] and with the WHO criteria,[3] be evaluated separately. The analysis suggested would be strongly biased by the fact that PVSG-classified patients have longer follow-up than WHO-classified patients. In the paper, we mentioned that the longer the follow-up, the higher the risk of transformation into myelofibrosis or leukemia. We regret that their request could not be satisfied, but a direct comparison of these two cohorts with different follow-up may give a misleading message. The second question from Thiele and Kvasnicka concerns the diagnostic differentiation between ET and prefibrotic/early fibrotic phase of primary myelofibrosis (PMF), an entity recognized on the basis of bone marrow features by the WHO classification of 2001.[4] However, the recent WHO classification requires the combination of histological picture, clonal markers and clinical parameters to diagnose PMF at prefibrotic or fibrotic phase.[3] In our series we excluded cases of PMF (excluded combination of leukoerythroblastosis, anemia, elevated LDH, spleen enlargement). Concerning the discussion on sequential bone marrow evaluations, we perform bone marrow biopsy at diagnosis in all the patients and during follow-up when we suspect clinical progression of the disease. We are glad to know that the prevalence of myelofibrosis reported by Thiele and Kvasnicka ranges between 2.8% and 3.5%. We find that this is a reassuringly low prevalence for patients with ET.

Francesco Passamonti,[1] Elisa Rumi,[1] Emanuela Boveri,[2] and Mario Lazzarino[1]

[1]Division of Hematology, and [2]Department of Surgical Pathology, Fondazione IRCCS Policlinico San Matteo, University of Pavia, Italy

Correspondence: Francesco Passamonti, Clinica Ematologica, Fondazione IRCCS Policlinico S. Matteo, viale Golgi 19, 27100 Pavia, Italy. E-mail: f.passamonti@smatteo.pv.it

Citation: Passamonti F, Rumi E, Boveri E, and Lazzarino M. Myelofibrotic transformation in essential thrombocythemia. Author reply. Haematologica 2009; 94: 433-433. doi:10.3324/haematol.2008.002071

References

1. Passamonti F, Rumi E, Arcaini L, Boveri E, Elena C, Pietra D, et al. Prognostic factors for thrombosis, myelofibrosis, and leukemia in essential thrombocythemia: a study of 605 patients. Haematologica 2008;93:1645-51.
2. Murphy S, Peterson P, Iland H, Laszlo J. Experience of the Polycythemia Vera Study Group with essential thrombocythemia: a final report on diagnostic criteria, survival, and leukemic transition by treatment. Semin Hematol 1997;34:29-39.
3. Tefferi A, Thiele J, Orazi A, et al. Proposals and rationale for revision of the World Health Organization diagnostic criteria for polycythemia vera, essential thrombocythemia, and primary myelofibrosis: recommendations from an ad hoc international expert panel. Blood 2007;110:1092-7.
4. Vardiman JW, Harris NL, Brunning RD. The World Health Organization (WHO) classification of the myeloid neoplasms. Blood 2002;100:2292-302.

A *JAK2*-V617F activating mutation in addition to KIT and FLT3 mutations is associated with clinical outcome in patients with t(8;21)(q22;q22) acute myeloid leukemia

A *JAK2*-V617F mutation was found in 3 of 45 (6.7%) patients with t(8;21) acute myeloid leukemia (AML), whereas only one of 137 (0.7%) patients with *de novo* AML other than t(8;21) had the same mutation (p=0.047). We examined the clinical significance of *KIT*, *FLT3* and *JAK2* mutations as a collective group. There was a significant difference in the cumulative incidence of relapse: 77% in the 21 patients with the mutations and 26% in 19 lacking mutations respectively (p=0.0083). Our study highlights the importance of *JAK2* mutations in addition to *KIT* and *FLT3* mutations as a prognostic factor in t(8;21) AML patients.

RUNX1(AML1)-RUNX1T1(MTG8) generated by t(8;21)(q22:q22) contributes to leukemic transformation, but additional events are required for full leukemogenesis.[1,2] Mutations in the receptor tyrosine kinases (RTK) including the *KIT* and *FLT3* genes are the genetic events that appear to cause acute myeloid leukemia (AML) harboring t(8;21) and are associated with unfavorable prognosis.[3,4] The activating missense mutation in the pseudokinase domain of the JAK2 cytoplasmic tyrosine kinase has been identified in a significant proportion of patients with myeloproliferative disorders.[5] Although the same somatic mutation has been found in a small number of AML patients, a relatively high incidence of *JAK2*-V617F mutation is often seen in *de novo* and therapy-related t(8;21) AML patients.[6-10] Nevertheless, whether *JAK2*-V617F mutation is associated with other biological parameters including clinical prognosis in patients with t(8;21) AML remains to be fully determined.

To examine its biological and prognostic impact, we studied the *JAK2* mutation in 45 patients with *de novo* t(8;21) AML. Approval for this study was obtained from the Institutional Review Board of Kumamoto University School of Medicine. The results of *KIT*, *FLT3*, *N-RAS*, *K-RAS* and *PDGFRα* mutations in 37 of the 45 patients have been reported previously.[3] Of the 45 patients, activating mutations in *KIT* and internal tandem duplications in *FLT3* were observed in 18 (40%) and 3 (6.7%) respectively. Mutations of *JAK2*-V617F were identified by allele specific RT-PCR and direct sequencing.[11] We detected the het-

erozygous *JAK2*-V617F mutation in 3 patients (6.7%) with t(8;21) AML, which was consistent with previous studies.[6-10] None of the 3 t(8;21) AML patients had a history of previous myeloproliferative disorders. No mutations other than V617F were found in the exons 12-14 of *JAK2*. Among 137 patients with *de novo* AML other than t(8;21), there was only one patient who had *JAK2* mutation (p=0.047). This patient had M2 with 46,XY,add(7)(q11),del(20)(q13). Thus, the present study confirmed that the *JAK2* mutation is highly associated with t(8;21) AML.

Although the occurrence of *KIT* and *FLT3* mutations was mutually exclusive in t(8;21) AML patients,[3] one patient harboring a *JAK2* mutation also had a KIT mutation and the other patient had a *K-RAS* mutation (Table 1). Although we cannot exclude the possibility that two different subclones in leukemic cells had each mutation, it is also likely that the same leukemic cells carry both mutations because heterozygous *JAK2* and *KIT* or *K-RAS* mutations are identified as equivocal peaks in the electropherogram of direct sequencing (*data not shown*). It is of note that a high prevalence of co-operating mutations of *FLT3*, *KIT*, or *N-RAS* in AML patients with the *JAK2* mutation has been reported.[7-9] In the current study, a total of 23 (51%) patients had mutations in *KIT*, *FLT3* and *JAK2*, suggesting that activating mutations in the *RTK* and *JAK2* play a critical role as a secondary event leading to the development of t(8;21) AML.

We examined the clinical significance of *KIT*, *FLT3* and *JAK2* mutations as a collective group because the present study was limited to a small number of *JAK2* mutated cases for the comparison of clinical features, and these mutations activate the same STAT signal transduction pathway and belong in the same class I mutation.[2] There was no significant relationship between the mutations and age, sex, leukocyte counts, platelet counts, CD56 expression, or additional chromosomal aberrations. However, t(8;21) AML patients with an activating mutation in *KIT*, *FLT3* and *JAK2* had significantly greater marrow blast percentages and serum lactate dehydrogenase levels than those without a mutation (*data not shown*). Considering that the *JAK2* mutation confers a proliferative and survival advantage on hematopoietic cells,[5] these clinical profiles appear to be associated with these mutations.

A total of 44 patients received intensive chemotherapy based on the Japan Adult Leukemia Study Group (JALSG) protocols in the AML87, AML89, AML92, AML95 and AML97 studies.[12] Although patients were treated with different schedules, all received regimens consisting of anthracyclines and cytarabine as induction therapy. Cytarabine plus one of the anthracyclines, high-dose cytarabine, or allogeneic hematopoietic stem cell transplantation (HSCT) was used as post-remission therapy. Patient 1 carrying both *KIT* and *JAK2* mutations did not respond to multiple induction chemotherapies including high-dose cytarabine therapy (Table 1). Patient 2 with the *JAK2* and *K-RAS* mutations achieved a complete remission (CR) but later relapsed. Patient 3 received allogeneic HSCT during the first CR and continued in CR. Twenty-one out of 23 (91%) patients with the mutations achieved CR, while 19 out of 21 (90%) patients lacking mutations obtained CR (p=0.9240). On the other hand, there was a significant difference in the cumulative incidence of relapse: 77% in the 21 patients with the mutations and 26% in 19 lacking mutations respectively (p=0.0083) (Figure 1A). It is likely that the poor outcome cannot be attributable only to *JAK2* mutation in patients with a *KIT* or *K-RAS* mutation although *JAK2* mutation together with other mutations may confer additive effects on the

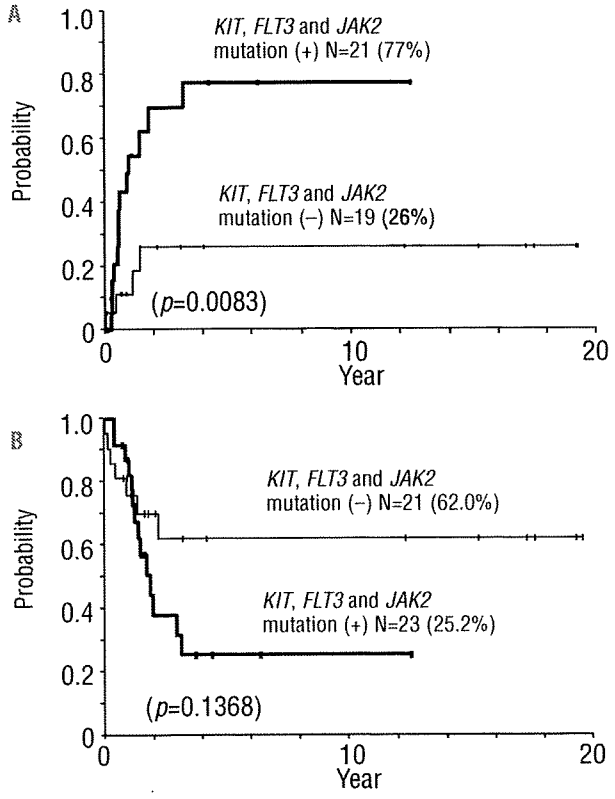

Figure 1. Cumulative incidence of relapse (A) and overall survival (B) in patients with t(8;21) acute myeloid leukemia by mutations in *KIT*, *FLT3* and *JAK2*. Estimation of survival distributions was performed using the Kaplan–Meier method and the differences were compared using the log-rank test.

Table 1. Clinical profiles of t(8;21) acute myeloid leukemia patients harboring the *JAK2* mutation.

Patient #	1	2	3
JAK2	V617F	V617F	V617F
KIT	N822Y	-	-
K-RAS	-	G12D	-
Age (years)	31	68	26
Sex	Male	Female	Female
Hemoglobin (g/dL)	6.9	8.1	7.1
Platelet (x10⁹/L)	13	57	15
Leukocyte (x10⁹/L)	43.9	30	32
Circulating blast (%)	35	18	78
Marrow blast (%)	22.5	40	NT
WBC index[a]	9.88	12	NT
LDH (U/L)[b]	1,829	2,398	1,120
CD56 expression	+	+	NT
Additional chromosome abnormality	add(7)(q22)	-	-X
Induction	Failure	CR	CR
Relapse-free survival (years)	0	1.4	12.0+
Overall survival (years)	1.3	1.8	12.0+

[a]Leukocyte count x marrow blast, [b]Normal range of lactate dehydrogenase is 112 - 213 U/L. NT: not tested, CR: complete remission.

clinical outcome. Illmer *et al.*[8] also showed that 4 of 5 t(8;21) or inv(16) AML patients with a *JAK2* mutation had early relapses within 20 months after diagnosis. Taken together, these results suggest that mutations in the *JAK2*, *KIT* and *FLT3* genes are associated with unfavorable clinical outcome in patients with t(8;21) AML.

Our study also implies that patients with *RTK* and *JAK2* mutations may benefit from allogeneic HSCT. Three patients with mutations received allogeneic HSCT after relapse and have achieved continuous second CR. Three patients in each group also received allogeneic HSCT at the first CR. As a consequence, 6 out of 9 patients with AML harboring *KIT*, *FLT3* and *JAK2* mutations who continued CR received allogeneic HSCT. When patients who underwent HSCT were censored at the date of the HSCT, the 6-year overall survival in patients with mutations was 25% compared to 62% in those without mutations (p=0.1368) (Figure 1B). These findings are of significant clinical import as activating mutations in *KIT*, *FLT3* and *JAK2* could be potential therapeutic targets for specific tyrosine kinase inhibitors and JAK2 pathway inhibitors in patients with t(8;21) AML harboring the mutations.

Eisaku Iwanaga, Tomoko Nanri, Naofumi Matsuno, Toshiro Kawakita, Hiroaki Mitsuya, and Norio Asou

Department of Hematology, Kumamoto University School of Medicine, Kumamoto, Japan

Key words: JAK2, KIT, FLT3, t(8;21), acute myeloid leukemia

Acknowledgments: this work was supported in part by Grants-in-Aid for Scientific Research from the Japanese Ministry of Education, Culture, Sport, Science and Technology, and Grants-in-Aid for Cancer Research from the Japanese Ministry of Health, Labor and Welfare.

Correspondence: Norio Asou, MD, Department of Hematology, Kumamoto University School of Medicine, 1-1-1 Honjo, Kumamoto 860-8556, Japan.
Phone: +81.96.373.5156, Fax: +81.96.363.5265.
E-mail: ketcnasou@gpo.kumamoto-u.ac.jp

Citation: Iwanaga E, Nanri T, Matsuno N, Kawakita T, Mitsuya H, and Asou N. A JAK2-V617F activating mutation in addition to KIT and FLT3 mutations is associated with clinical outcome in patients with t(8;21)(q22;q22) acute myeloid leukemia. Haematologica 2009; 94:433-435. doi: 10.3324/haematol.13283

References

1. Asou N. The role of a Runt domain transcription factor AML1/RUNX1 in leukemogenesis and its clinical implications. Crit Rev Oncol Hematol 2003;45:129-50.
2. Kuchenbauer F, Schnittger S, Look T, Gilliland G, Tenen D, Haferlach T, et al. Identification of additional cytogenetic and molecular genetic abnormalities in acute myeloid leukaemia with t(8;21)/AML1-ETO. Br J Haematol 2006; 134:616-9.
3. Nanri T, Matsuno N, Kawakita T, Suzushima H, Kawano F, Mitsuya H, et al. Mutations in the receptor tyrosine kinase pathway are associated with clinical outcome in patients with acute myeloblastic leukemia harboring t(8;21) (q22;q22). Leukemia 2005;19:1361-6.
4. Cairoli R, Beghini A, Grillo G, Nadali G, Elice F, Ripamonti CB, et al. Prognostic impact of c-KIT mutations in core binding factor leukemias: an Italian retrospective study. Blood 2006;107:3463-8.
5. Ihle JN, Gilliland DG. Jak2: normal function and role in hematopoietic disorders. Curr Opin Genet Dev 2007;17:8-14.
6. Lee JW, Kim YG, Soung YH, Han KJ, Kim SY, Rhim HS, et al. The JAK2 V617F mutation in de novo acute myelogenous leukemias. Oncogene 2006;25:1434-6.
7. Döhner K, Du J, Corbacioglu A, Scholl C, Schlenk RF, Döhner H. JAK2V617F mutations as cooperative genetic lesions in t(8;21)-positive acute myeloid leukemia. Haematologica 2006;91:1569-70.
8. Illmer T, Schaich M, Ehninger G, Thiede C. Tyrosine kinase mutations of JAK2 are rare events in AML but influence prognosis of patients with CBF-leukemias. Haematologica 2007;92:137-8.
9. Vicente C, Vázquez I, Marcotegui N, Conchillo A, Carranza C, Rivell G, et al. JAK2-V617F activating mutation in acute myeloid leukemia: prognostic impact and association with other molecular markers. Leukemia 2007; 21:2386-90.
10. Schnittger S, Bacher U, Kern W, Haferlach C, Haferlach T. JAK2 seems to be a typical cooperating mutation in therapy-related t(8;21)/ AML1-ETO-positive AML. Leukemia 2007;21:183-4.
11. Heller PG, Lev PR, Salim JP, Kornblihtt LI, Goette NP, Chazarreta CD, et al. JAK2V617F mutation in platelets from essential thrombocythemia patients: correlation with clinical features and analysis of STAT5 phosphorylation status. Eur J Haematol 2006;77:210-6.
12. Miyawaki S, Sakamaki H, Ohtake S, Emi N, Yagasaki F, Mitani K, et al. A randomized, postremission comparison of four courses of standard-dose consolidation therapy without maintenance therapy versus three courses of standard-dose consolidation with maintenance therapy in adults with acute myeloid leukemia: the Japan Adult Leukemia Study Group AML 97 Study. Cancer 2005;104: 2726-34.

JAK1 mutation analysis in T-cell acute lymphoblastic leukemia cell lines

T-cell acute lymphoblastic leukemia (T-ALL) is a malignancy of T-cell precursors that mainly occurs in children and adolescents. A variety of oncogenic events that are involved in the pathogenesis of T-ALL have been identified, including *NOTCH1* and *PTEN* mutations, overexpression of *TAL1*, *LYL1* and *TLX1*, and deletion of *CDKN2A* (p16).[1] Apart from mutations in *FLT3* and *NRAS*, and chromosomal aberrations generating the NUP214-ABL1 fusion, mutations that drive proliferation and survival of T-ALL cells are still unknown in the majority of patients. Recently, activating point mutations in the *JAK1* gene were identified in patients with ALL, and rarely also in acute myeloid leukemia (AML) patients.[2-4] In T-ALL, *JAK1* mutations were identified in approximately 20% of adult T-ALL cases, with a much lower frequency in childhood T-ALL.[2] These mutations are very heterogeneous in the sense that they are dispersed over several *JAK1* domains, and differ in their ability to transform hematopoietic cells and to activate downstream signaling pathways such as the STAT, PI3K and MAPK cascades.[2-4]

Leukemia cell lines with mutations in *FLT3*, *JAK2* and *NOTCH1* have been described as useful models for preclinical testing of small molecule inhibitors.[5-8] Given the recent identification of *JAK1* mutations in T-ALL, we investigated if *JAK1* mutations could be detected in a panel of 18 common T-ALL cell lines. By sequencing of the JAK1 open reading frame at cDNA level in these cell lines, we identified 2 transcript variants, one non-synonymous substitution, as well as several synonymous substitutions (Table 1).

A first transcript variant was identified in the HPB-ALL cell line (Figure 1A, 1B). This transcript lacks nucleotides 2896-2967, encoding amino acids 966-989 that are located between the P-loop and the activation loop in the kinase domain. When sequencing HPB-ALL genomic DNA, we could not detect the presence of a deletion, but we detected a single nucleotide change (2897 A>T) generating a novel GT splice donor site in

KW-2449, a novel multikinase inhibitor, suppresses the growth of leukemia cells with FLT3 mutations or T315I-mutated *BCR/ABL* translocation

*Yukimasa Shiotsu,[1] *Hitoshi Kiyoi,[2] Yuichi Ishikawa,[2,3] Ryohei Tanizaki,[3] Makiko Shimizu,[1] Hiroshi Umehara,[1] Kenichi Ishii,[1] Yumiko Mori,[2,3] Kazutaka Ozeki,[2] Yosuke Minami,[3] Akihiro Abe,[3] Hiroshi Maeda,[4] Tadakazu Akiyama,[1] Yutaka Kanda,[1] Yuko Sato,[5] Shiro Akinaga,[4] and Tomoki Naoe[3]

[1]Fuji Research Park, Kyowa Hakko Kirin, Shizuoka; [2]Department of Infectious Diseases and [3]Department of Hematology and Oncology, Nagoya University Graduate School of Medicine, Nagoya; [4]Clinical Development Division, Kyowa Hakko Kirin, Tokyo; and [5]Research Institute, International Medical Center of Japan, Tokyo, Japan

KW-2449, a multikinase inhibitor of FLT3, ABL, ABL-T315I, and Aurora kinase, is under investigation to treat leukemia patients. In this study, we examined its possible modes of action for antileukemic effects on FLT3-activated, FLT3 wild-type, or imatinib-resistant leukemia cells. KW-2449 showed the potent growth inhibitory effects on leukemia cells with FLT3 mutations by inhibition of the FLT3 kinase, resulting in the down-regulation of phosphorylated-FLT3/STAT5, G_1 arrest, and apoptosis. Oral administration of KW-2449 showed dose-dependent and significant tumor growth inhibition in FLT3-mutated xenograft model with minimum bone marrow suppression. In FLT3 wild-type human leukemia, it induced the reduction of phosphorylated histone H3, G_2/M arrest, and apoptosis. In imatinib-resistant leukemia, KW-2449 contributed to release of the resistance by the simultaneous down-regulation of BCR/ABL and Aurora kinases. Furthermore, the antiproliferative activity of KW-2449 was confirmed in primary samples from AML and imatinib-resistant patients. The inhibitory activity of KW-2449 is not affected by the presence of human plasma protein, such as α1-acid glycoprotein. These results indicate KW-2449 has potent growth inhibitory activity against various types of leukemia by several mechanisms of action. Our studies indicate KW-2449 has significant activity and warrants clinical study in leukemia patients with FLT3 mutations as well as imatinib-resistant mutations. (Blood. 2009;114:1607-1617)

Introduction

Overexpression and activating mutations of protein tyrosine kinases (PTK) are frequently observed in several kinds of hematologic malignancies.[1,2] Abnormally activated PTK-mediated signal transduction pathways are involved in their pathogenesis, such as autonomous proliferation, antiapoptosis, and differentiation block. The remarkable clinical success of the ABL kinase inhibitor, imatinib mesylate (IM), in the treatment of BCR/ABL-positive chronic myeloid leukemia (CML) and acute lymphoblastic leukemia (ALL) has proved the principle of molecularly targeted therapy.[3,4] Therapeutic intervention targeting PTKs is therefore highly expected to improve prognosis of patients with hematologic malignancy. FMS-like receptor tyrosine kinase (FLT3) is a class III receptor tyrosine kinase together with cKIT, FMS, and PDGFR.[5,6] FLT3 mutations were first reported as internal tandem duplication (FLT3/ITD) of the juxtamembrane domain-coding sequence; subsequently, a missense point mutation at the Asp835 residue and point mutations, deletions, and insertions in the codons surrounding Asp835 within a tyrosine kinase domain of FLT3 (FLT3/KDM) have been found.[7,8] FLT3 mutation is the most frequent genetic alteration in acute myeloid leukemia (AML) and involved in the signaling pathway of proliferation and survival in leukemia cells.[5,6] Several large-scale studies have confirmed that FLT3/ITD is strongly associated with leukocytosis and a poor prognosis.[9] In addition to FLT3 mutation, overexpression of FLT3 is an unfavorable prognostic factor for overall survival in AML, and it has been revealed that overexpressed FLT3 had the same sensitivity to the FLT3 inhibitor as FLT3/ITD.[10] Because high-dose chemotherapy and stem cell transplantation cannot conquer the adverse effects of FLT3 mutations, it is expected that the development of FLT3 kinase inhibitors will make more efficacious therapeutic strategy for leukemia therapy.[11,12] To date, several small-molecule tyrosine kinase inhibitors have been shown to have a potency to inhibit the FLT3 kinase, and several of them, such as CEP-701, PKC412, MLN-518, and SU11248, have been subjected to clinical trials.[13-16] However, the clinical efficacy of these FLT3 inhibitors for AML with FLT3 mutations is limited to the transient clearance of leukemia blast cells as a single agent; thus, the therapeutic strategy of some FLT3 inhibitors moves toward a combination with conventional chemotherapy.[17] This move is a logical step based on the in vitro evidence of the synergy with conventional cytotoxic agents,[18,19] although it should be considered that several problems regarding adverse effects and pharmacokinetics have been apparent from clinical trials of monotherapy.[20] Furthermore, because acute leukemia is a complex multigenetic disorder,[21-23] a simultaneous inhibition of multiple protein kinases is thought to be advantageous over the increasing potency against the selective kinases. Recent high-throughput resequencing of TK in AML samples revealed new somatic mutations of JAK1, DDR1, and NRTK1 in addition to

Submitted January 13, 2009; accepted May 28, 2009. Prepublished online as *Blood* First Edition paper, June 18, 2009; DOI 10.1182/blood-2009-01-199307.

*Y. Shiotsu and H.K. contributed equally to this study.

The publication costs of this article were defrayed in part by page charge payment. Therefore, and solely to indicate this fact, this article is hereby marked "advertisement" in accordance with 18 USC section 1734.

previously well-known FLT3, cKit, JAK2, and FGFR mutations.[24,25] These observations collectively indicate that FLT3 inhibitors in the next generation should have an adequately balanced potency against key oncogenic kinases, which are responsible for the disease progression and/or the resistance to standard therapeutics. Here we describe efficacy of a novel small-molecule protein kinase inhibitor, KW-2449, which has a potent and unique kinase inhibition profile against FLT3, ABL, T315I-mutant ABL (ABL-T315I) tyrosine kinases as well as Aurora kinase.

Methods

Kinase inhibition profile

The in vitro kinase assays were performed according to the KinaseProfiler Assay Protocols of Upstate Biotechnology.

Growth inhibition profile cell-cycle analysis

FLT3/ITD-, FLT3/D835Y-expressing, wt-FLT3/FL-coexpressing, and FLT3/ITD-green fluorescent protein (GFP)–expressing murine myeloid-progenitor 32D cells were previously reported.[26] Human leukemia cell line MOLM-13 was obtained from DSMZ (German Resource Center for Biological Material); MV4;11, RS4;11, K562, and HL60 from ATCC. Wt-BCR/ABL-positive human ALL cell line TCC-Y and its IM-resistant clones, TCC-Y/sr cells, which has the T315I-mutated BCR/ABL, were reported previously.[27] Cell viability was determined by the sodium 3′-[1-(phenylaminocarbonyl)-3, 4-tetrazolium]-bis (4-methoxy-6-nitro) benzene sulfonic acid hydrate assay after incubation with or without KW-2449 for 72 hours at 37°C. The number of viable cells was determined using the Cell Proliferation Kit II (Roche Diagnostics). For cell-cycle analysis, MOLM-13 and RS4;11 cells were treated with KW-2449. After 24, 48, and 72 hours of incubation at 37°C, DNA contents were analyzed as previously described.[28] Cell cycle distribution of K562, TCC-Y, and TCC/Ysr was analyzed 24 hours after treatment with KW-2449 or imatinib.

Effects of hAGP on growth inhibitory activity by FLT3 inhibitors

MOLM-13 cells were incubated with various concentrations of KW-2449, PKC-412, and CEP-701 in the presence of 0.1% of human α1-acid glycoprotein (hAGP; Sigma-Aldrich). Cell viability was determined by sodium 3′-[1-(phenylaminocarbonyl)-3, 4-tetrazolium]-bis (4-methoxy-6-nitro) benzene sulfonic acid hydrate assay after incubation for 72 hours at 37°C.

Western blot

MOLM-13 cells were treated with KW-2449 for 24 hours, and cell pellets were suspended with lysis buffer. FLT3 proteins were immunoprecipitated with anti-FLT3 antibody (S18; Santa Cruz Biotechnology). The precipitated samples were separated by sodium dodecyl sulfate–polyacrylamide gel electrophoresis (SDS-PAGE), and electroblotted onto Immobilon polyvinylidene difluoride membranes (Millipore). Immunoblotting was performed with antiphosphotyrosine antibody (4G10; Upstate Biotechnology). The membranes were incubated with the stripping buffer and then reprobed with anti-FLT3 antibody (C20; Santa Cruz Biotechnology). Signals were developed using an enhanced chemiluminescence system (GE Healthcare). To examine the phosphorylation level of STAT5, whole cell lysates were subjected to immunoblotting with antiphospho-STAT5 antibody (Kyowa Hakko Kogyo). The membranes were incubated with the stripping buffer and then reprobed with anti-STAT5 antibody (Santa Cruz Biotechnology).

RS4;11 cells were suspended in culture medium containing nocodazole with or without KW-2449. After a 30-minute incubation, cells were harvested and cell pellets were suspended in lysis buffer. Whole cell lysates were subjected to immunoblotting with antiphospho-HH3 (Ser10) antibody (Upstate Biotechnology). The membranes were incubated with the stripping buffer and then reprobed with anti-HH3 antibody (Cell Signaling).

Concentration of KW-2449 in plasma and tumors

Severe combined immunodeficiency (SCID) mice (Fox CHASE C.B-17/Icr-scidJcl, male, 5 weeks old) were purchased from CLEA Japan. Mice were treated with an intraperitoneal injection of antiasialo GM1 antibody (0.3 mg/mouse, Wako Pure Chemical Industries). The day after antiasialo GM1 antibody treatment, all mice were subcutaneously inoculated in the shaved area with 10^7 of MOLM-13 cells. Ten days after inoculation, KW-2449 at 20 mg/kg was orally administered to mice twice. Blood and tumor samples were collected 4, 8, 12, and 24 hours after the second administration. The plasma and tumor samples were analyzed to measure KW-2449 concentration with liquid chromatography–mass spectrometry–mass spectrometry (LC/MS/MS).

In vivo antileukemia effects on xenograft transplantation

SCID mice were subcutaneously inoculated with MOLM-13 cells. Five days after inoculation, tumor volume was measured using the Antitumor test system II (Human Life). The 25 mice with tumors ranging from 90 to 130 mm^3 were selected and randomized using the Antitumor test system II. From the day of randomization, vehicle (0.5 wt/vol% MC400) or KW-2449 (2.5, 5.0, 10, and 20 mg/kg) was orally administered to mice twice a day for 14 days. Tumor volume was measured twice a week during the treatment.

In vivo antileukemia effects on syngeneic transplantation

C3H/Hej mice were purchased from Charles River Japan. Fifteen C3H/Hej mice were intravenously inoculated with 2×10^6 of FLT3/ITD-GFP-32D cells and then randomly divided into 3 groups of 5 mice each. On the seventh day after inoculation, peripheral blood (PB) was collected from the mice. From the 10th day after inoculation, mice were treated with KW-2449 at 40 mg/kg (orally) twice a day, cytosine arabinoside (AraC) at 150 mg/kg (intravenously) daily, or vehicle for 4 days. Six hours after the last administration, PB was collected. Total RNA was extracted from each PB sample using a QIAamp RNA Blood Mini Kit (QIAGEN). cDNA was synthesized from each RNA sample using a random primer and Moloney murine leukemia virus reverse transcriptase (Super-Script II; Invitrogen) according to the manufacturer's recommendations. The expression level of the human FLT3 transcript was quantitated using a real-time fluorescence detection method on an ABI Prism 7000 sequence detection system (Applied Biosystems) as previously reported.[10] After the collection of PB, spleens and bone marrow (BM) cells from femora were collected, and the total cell number from each femur was counted using a cell counter. To discriminate the FLT3/ITD-GFP-32D leukemia cells and normal BM cells, all collected cells were subjected to flow cytometry analysis after phycoerythrin-conjugated antihuman FLT3 monoclonal antibody (SF1.340; Immunotech) staining. In this flow cytometry analysis, GFP-positive cells were defined as residual leukemia in the femur. The weight of each collected spleen was measured.

Primary patient samples

BM samples from patients with AML or CML in blast crisis were subjected to Ficoll-Hypaque (Pharmacia LKB) density gradient centrifugation. All samples were morphologically confirmed to contain more than 90% leukemia cells after centrifugation on May-Grünwald Giemsa-stained cytospin slides, and then cryopreserved in liquid nitrogen before use. Informed consent was obtained from all patients in accordance with the Declaration of Helsinki to use their samples for the present study as well as banking and molecular analysis, and approval was obtained from the ethics committees of Nagoya University and Ogaki Municipal Hospital for this study. Mutations of the FLT3 gene were examined as previously reported.[8] Primary AML cells were incubated with RPMI1640 medium containing 10% fetal calf serum and 0.1 μM KW-2449 for 6 hours, and cell pellets were suspended with lysis buffer. Whole cell lysates were subjected to immunoblotting with antiphospho-FLT3 (Tyr591) (Cell Signaling Technology) and antiphospho-STAT5 antibodies. The membranes were incubated with the stripping buffer and then reprobed with anti-FLT3 (C20; Santa Cruz Biotechnology) and anti-STAT5 antibodies (Santa Cruz Biotechnology).

Colony formation analysis

Human AML cells (10^5 cells) were plated in MethoCult methylcellulose semisolid medium containing human stem cell factor, granulocyte-macrophage colony-stimulating factor (GM-CSF), and interleukin-3 (H4534; Stem Cell Technologies) with or without KW-2449 (0.1 μM) and then incubated at 37°C for 14 days. Colonies with more than 20 cells were scored using an inverted microscope.

Human cord blood (CB) was collected after full-term deliveries with informed consent obtained in accordance with the Declaration of Helsinki and approved by the Review Board of Tokai Cord Blood Bank. Mononuclear cells were collected by the Ficoll-Hypaque (Pharmacia LKB) density gradient centrifugation. CB mononuclear cells (5×10^4 cells) were plated in complete MethoCult methylcellulose medium (H4435; Stem Cell Technologies) with an increasing concentration of KW-2449. After 14 days in culture, erythroid burst-forming units (BFU-E), colony-forming unit–granulocyte macrophage (CFU-GM), and colony-forming unit–granulocyte, erythrocyte, monocyte/macrophage, megakaryocyte (CFU-GEMM) colonies were counted.

Inhibitory effects on BCR/ABL-positive leukemia cells

K562, TCC-Y, and TCC/Ysr cells were incubated with an increasing concentration of KW-2449 or imatinib for 72 hours, and cell pellets were suspended with lysis buffer. Whole cell lysates were subjected to immunoblotting with antiphospho-ABL (Tyr245; Cell Signaling Technology), antiphospho-STAT5, and anti-poly(ADP-ribose) polymerase (PARP; Cell Signaling Technology) antibodies.

Human CML in blast crisis (CML-BC) cells with T315I-mutation were intravenously inoculated into nonobese diabetic (NOD)/SCID mice (CLEA Japan). On the 28th day after the inoculation, engraftment of leukemia cells in each mouse was confirmed by the detection of human CD45-positive cells in PB. On the next day, PB was collected from the leukemia cell-engrafted mice, and then the mice were treated with KW-2449 at 20 mg/kg twice a day, IM at 150 mg/kg daily, or vehicle for 5 days. Twelve hours after the last administration, PB was collected from each mouse. Total RNA was extracted from each PB sample, and cDNA was synthesized from each RNA sample using a random primer and Moloney murine leukemia virus reverse transcriptase as described in "In vivo antileukemia effects on syngeneic transplantation." The expression level of the BCR/ABL transcript was quantitated using a real-time fluorescence detection method as previously reported.[29] The *GAPDH* served as a control for cDNA quality. Relative gene expression levels were calculated using standard curves and adjusted based on the expression level of the *GAPDH* gene.

After the collection of PB, femora were subjected to pathologic examination. Residual leukemia cells were evaluated by the immunohistochemical staining with antihuman CD45 antibody (Dako North America) as previously reported.[30] The animal experiments were approved by the institutional ethics committee for Laboratory Animal Research, Nagoya University School of Medicine and performed according to the guidelines of the institute.

Statistical analysis

Differences in continuous variables were analyzed with the Mann-Whitney U test for distribution among 2 groups or the Bonferroni test for distribution among more than 3 groups. Differences in therapeutic effects were analyzed with the repeated-measures analysis of variance method. These statistical analyses were performed with the StatView-J 5.0 software (Abacus Concepts).

Results

Development of KW-2449 and its kinase inhibition profile

Our aim was to generate an orally available and highly potent FLT3 inhibitor with low toxicity profile for leukemia patients. For this goal, we screened the chemical libraries of Kyowa Hakko Kirin (previously Kyowa Hakko Kogyo) using several leukemia cells, which have several activated mutations in FLT3 or BCR-ABL translocation. As a result, we identified several chemo-types with different kinase inhibition profiles, intensively studied the structures of the identified chemo-types to improve the potency and selectivity, and then finally generated KW-2449 (Figure 1A).

KW-2449 inhibited FLT3 and ABL kinases with half-maximal inhibitory concentration (IC_{50}) values of 0.0066 and 0.014 μM, respectively. In addition, it potently inhibited ABL-T315I, which is associated with IM resistance, with an IC_{50} value of 0.004 μM. On the other hand, KW-2449 had little effect on PDGFRβ, IGF-1R, EGFR, and various serine/threonine kinases even at a concentration of 1 μM. Among various serine/threonine kinases examined, KW-2449 inhibited Aurora A kinase with IC_{50} of 0.048 μM (Table 1) and Aurora B kinase with the equivalent potency (data not shown).

In vitro effects of KW-2449 on FLT3 mutated leukemia

In vitro kinase inhibition profile of KW-2449 indicated its extreme potency against FLT3 kinase. We first examined the effects of KW-2449 on several human leukemia cell lines with activated FLT3 and mutant FLT3-transfected cells. Because constitutive activation of FLT3 in leukemia cells is reportedly induced by mutation or coexpression of wild-type FLT3 (wt-FLT3) and FLT3 ligand (FL), we evaluated the growth inhibitory effect on mutant FLT3 (FLT3/ITD or FLT3/D835Y)–expressing and wt-FLT3– and FL-coexpressing (wt-FLT3/FL) murine myeloid-progenitor 32D cells. In addition, we evaluated the efficacy against FLT3/ITD-harboring human AML cell lines, MOLM-13 and MV4;11. Previously, we confirmed that FLT3 kinase is constitutively activated in these cell lines, and FI-700, a FLT3 selective inhibitor, can suppress the growth of mutated FLT3 transfected 32D cells as well as MOLM-13 and MV4;11 cells.[31] As expected, KW-2449 showed growth inhibitory activities against FLT3/ITD-, FLT3/D835Y-, and wt-FLT3/FL-expressing 32D cells, MOLM-13 and MV4;11 with half-maximal growth inhibitory concentration (GI_{50}) values of 0.024, 0.046, 0.014, 0.024, and 0.011 μM, respectively (Table 2). These results indicate that KW-2449 has the potent growth inhibitory activities against not only FLT3/ITD-expressing leukemia cells but also FLT3/KDM-activated and wild-type FLT3-overexpressing leukemia cells.

It has been reported that PKC-412 and CEP-701, whose chemical structure contains indolocarbazole, tightly bind to hAGP. Although these compounds have been in clinical investigation as FLT3 inhibitors, the significant reduction of their inhibitory activity caused by tight hAGP binding is in part associated with the limited clinical efficacy despite their long exposure in vivo, as well as the potency in vitro.[32,33] In these circumstances, we selected the compounds whose cellular efficacy was not attenuated by the presence of hAGP. Indeed, an addition of hAGP to culture media reduced the growth inhibitory effect of PKC-412 and CEP-701 more than 100- to 1000-fold, whereas the growth inhibitory activity of KW-2449 was not attenuated by hAGP (Figure 1E).

In accordance with growth inhibitory effect, KW-2449 suppressed the phosphorylations of FLT3 (P-FLT3) and its downstream molecule phospho-STAT5 (P-STAT5) in MOLM-13 cells in a dose-dependent manner (Figure 1B). Furthermore, KW-2449 increased the percentage of cells in the G_1 phase of the cell cycle and reciprocally reduced the percentage of cells in the S phase, resulting in the increase of apoptotic cell population (Figure 1C-D). These results indicated that the dephosphorylation of constitutively active FLT3 kinase by KW-2449 induced the G_1 arrest to leukemia

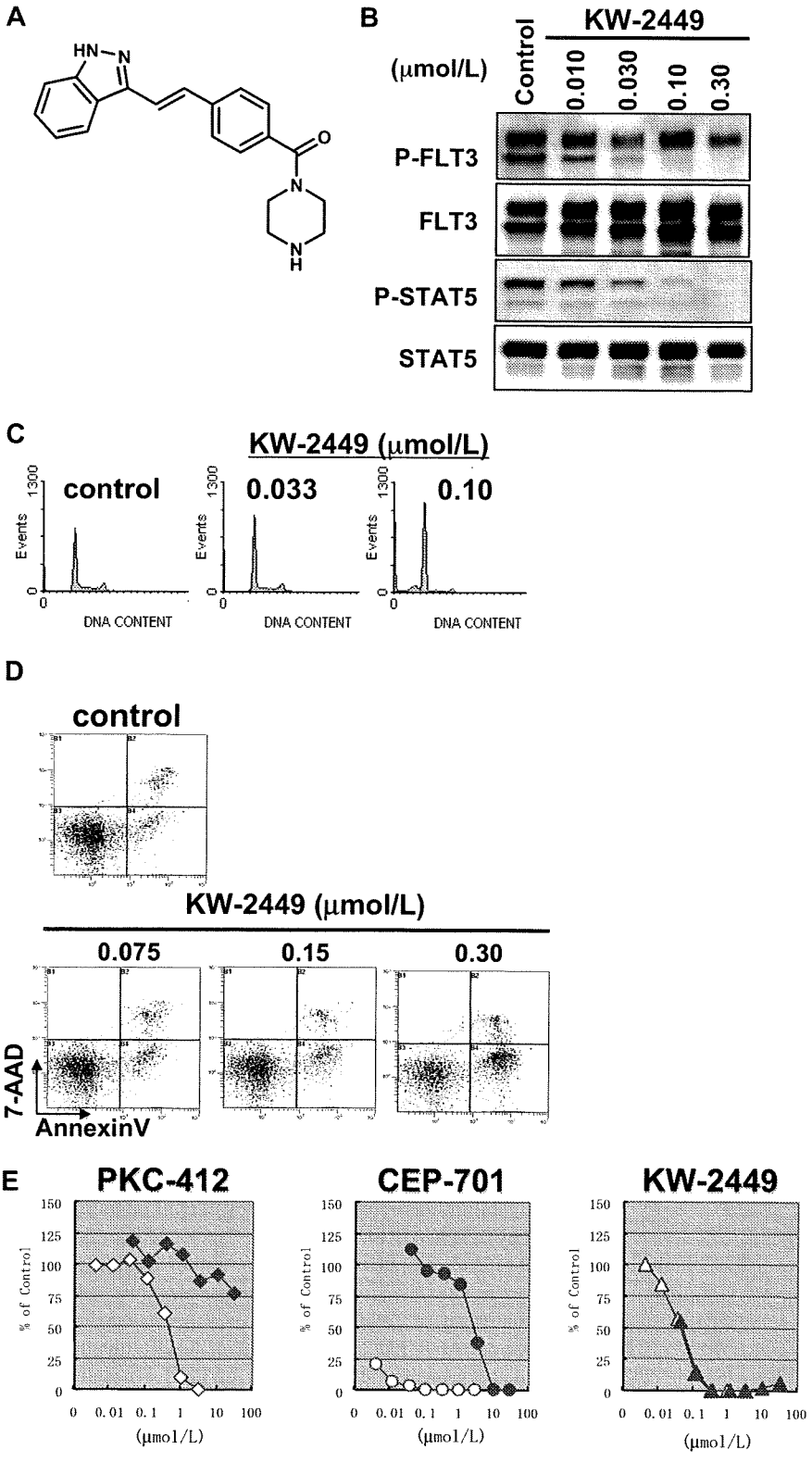

Figure 1. Effects of KW-2449 on human leukemia cells with FLT3 mutation. (A) Chemical structure of KW-2449. (B) MOLM-13 cells, which express FLT3/ITD, were treated with KW-2449 at the indicated concentrations for 24 hours. For analysis of FLT3 and its phosphorylated form (P-FLT3), the blots of immunoprecipitated FLT3 SDS-PAGE samples were analyzed by antiphosphotyrosine (P-Tyr) antibody and anti-FLT3 antibody. For detection of STAT5 and its phosphorylated form (P-STAT5), total cell lysate SDS-PAGE samples were analyzed by anti-P-STAT5 antibody and anti-STAT5 antibody as primary antibodies. Phosphorylation levels of FLT3 and STAT5 were decreased by KW-2449 in a dose-dependent manner. (C) MOLM-13 cells were treated with various concentrations of KW-2449 for 48 hours, and cell-cycle distribution was analyzed as described in "Growth inhibition profile and cell-cycle analysis." (D) MOLM-13 cells were treated with various concentrations of KW-2449 for 48 hours, and apoptosis induction was analyzed by 7-amino-actinomycin D/annexin V staining. (E) Inhibitory effects of hAGP on growth inhibitory activity against MOLM-13 cells were compared between KW-2449 and potent FLT3 inhibitors, PKC-412 and CEP-701, as described in "Effects of hAGP on growth inhibitory activity by FLT3 inhibitors." Growth inhibitory activity of KW-2449 was not affected by the presence of hAGP.

cells with FLT3 activation, resulting in apoptosis. Apparent increase of sub-G_1 apoptotic cells was also observed after KW-2449 exposure over 0.10 μM, at which concentration complete down-regulation of P-FLT3 was observed.

To confirm these effects on primary leukemia, we further analyzed the activities of KW-2449 using 10 human primary AML cells that consisted of 5 AML with wt-FLT3: 4 with FLT3/ITD and 1 with both FLT3/ITD and FLT3/KDM. In all AML cases with FLT3 mutation, KW-2449 (0.1 μM) reduced the phosphorylation levels both of FLT3 and STAT5 (Figure 2A). In accordance with the dephosphorylation level, the colony formations of AML cases with FLT3 mutation were inhibited by KW-2449 (Figure 2B). In contrast, the inhibitory effect of KW-2449 on the colony formations of all AML cases with wt-FLT3 was minimal at 0.1 μM

Table 1. Kinase inhibitory profile of KW-2449

Kinase	KW-2449
Tyrosine kinase	
FLT3	0.0066
FLT3/D835Y	0.001
KIT	0.30
PDFGRα	1.7
ABL	0.014
ABL-T315I	0.004
SRC	0.40
JAK2	0.15
FGFR1	0.036
Serine/threonine kinase	
Aurora A	0.048

In vitro kinase inhibition IC_{50} (μmol/L). IC_{50} values of KW-2449 were determined by in vitro kinase assays as described in "Kinase inhibition profile."

(Figure 2B). In 2 cases with wt-FLT3 (Wt-3 and Wt-5), constitutive phosphorylations of FLT3 were observed, although KW-2449 did not inhibit their colony formations. In the Wt-3 case, the weak inhibitory effect on P-FLT3 might reflect the minimum effect on the colony formation. However, in the Wt-5 case, KW-2449 significantly reduced the level of P-FLT3, whereas the colony formation was not inhibited. In this case, constitutive phosphorylation of STAT5 was also observed, although KW-2449 did not reduce its phosphorylation level, indicating that the STAT5 was phosphorylated by another kinase signal. These results therefore suggested that KW-2449 can dephosphorylate constitutively active wt-FLT3 kinase but not inhibit the proliferation of leukemia cells if they were not mainly addicted to FLT3 the kinase.

The inhibitory effect of KW-2449 on normal hematopoiesis was also evaluated using human hematopoietic progenitors. Mononuclear cells from 5 independent CB were plated in complete methylcellulose semisolid medium with an increasing concentration of KW-2449. Although KW-2449 inhibited the colony formation of CB mononuclear cells in a dose-dependent manner, the distribution of BFU-E, CFU-GM, and CFU-GEMM colonies was not affected by the KW-2449 treatment (Figure 2C-D). The Bonferroni test revealed that statistically significant differences in the total number of colonies were found between control and at the 0.5 μM ($P < .01$) concentration, and at the 0.01 μM and at the 0.5 μM ($P < .05$) concentration. The reduction of a total colony number was at most 59.6% plus or minus 20.2% of the control, at 0.1 μM of KW-2449. These results indicated that the suppressive effect of KW-2449 on the normal hematopiesis was modest, whereas that on leukemia with FLT3 mutations was significant (Figure 2B-C).

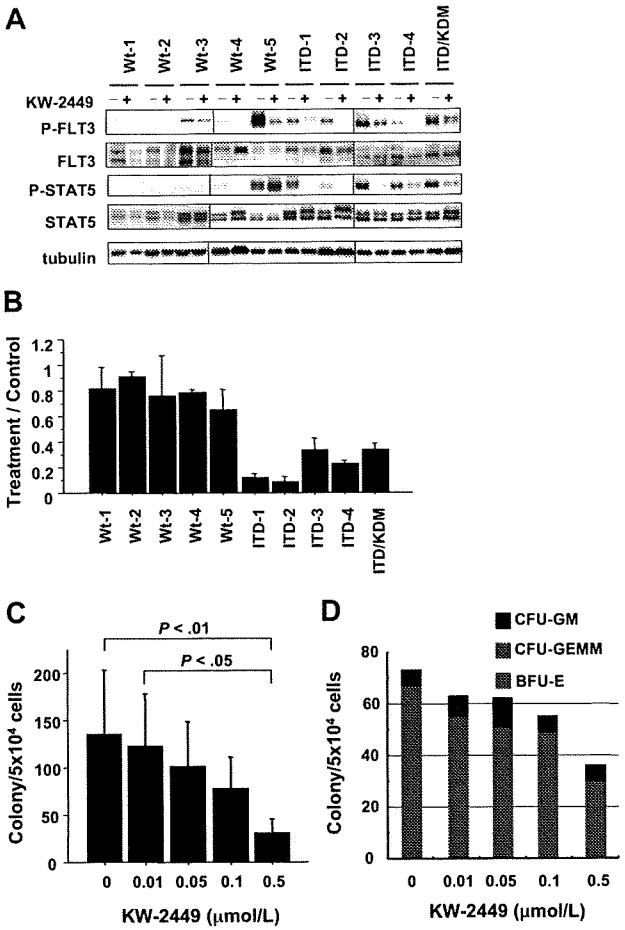

Figure 2. Inhibitory effects of KW-2449 on primary AML and colony-forming cells. (A) Ten AML samples consisting of 5 with wild-type FLT3 (Wt-1 to Wt-5), 3 with FLT3/ITD (ITD-1 to ITD-4), and one with both FLT3/ITD and FLT3/KDM (ITD/KDM), were analyzed. Primary AML cells were incubated with or without KW-2449 at 0.1 μM for 6 hours, and then phosphorylation status of FLT3 and STAT5 was analyzed. KW-2449 reduced phosphorylation levels of FLT3 and STAT5 in all AML samples with *FLT3* mutations. In the Wt-5 sample, KW-2449 reduced the phosphorylation level of FLT3 but not of STAT5. Vertical lines have been inserted to indicate a repositioned gel lane. (B) AML cells were suspended in methylcellulose semisolid medium containing human stem cell factor, GM-CSF, and interleukin-3 with or without 0.1 μM KW-2449. Colonies were counted after 14 days. Mean treatment/control ratio ± SD from 3 experiments in each sample are shown. In accordance with the down-regulation levels of FLT3 and STAT5 phosphorylations, KW-2449 inhibited the colony formations in all AML samples with FLT3 mutations. In the Wt-5 sample, weak inhibition of the colony formation seems to reflect the sustained STAT5 activation induced by another activation mechanism. (C) Mononuclear cells from human CB were plated in the complete methylcellulose semisolid medium with an increasing concentration of KW-2449. After 14 days of culture, BFU-E, CFU-GM, and CFU-GEMM colonies were counted. Mean total colony numbers ± SD at the indicated concentrations of KW-2449 are shown (n = 5). Although KW-2449 inhibited a total number of colonies in a dose-dependent manner, the Bonferroni test revealed that the statistical significances were found between control and at the 0.5 μM ($P < .01$), and at the .01 μM and at the 0.5 μM ($P < .05$). (D) The representative result of the distribution of BFU-E, CFU-GM, and CFU-GEMM colonies from 1 CB sample is shown. Although KW-2449 inhibited the colony formation of CB mononuclear cells in a dose-dependent manner, the distribution of BFU-E, CFU-GM, and CFU-GEMM colonies was not affected by the KW-2449 treatment.

Table 2. Growth inhibitory profile of KW-2449

Cell lines	KW-2449	Imatinib
32D transfectant		
Mock (with IL-3)	> 10	—
FLT3/ITD	0.024	—
FLT3/D835Y	0.046	—
Wt-FLT3/FL	0.014	—
Human leukemia		
MOLM-13	0.024	> 10
MV4;11	0.011	—
RS4;11	0.23	20
HL-60	0.65	> 10
BCR/ABL+ leukemia		
K562	0.27	0.24
TCC-Y	0.49	0.18
TCC-Y/sr	0.42	24

Growth inhibition GI_{50} (μmol/L). GI_{50} values of KW-2449 and imatinib were determined by in vitro XTT assays. MOLM-13 and MV4;11 cells had FLT3/ITD. K562 and TCC-Y cells had wt-BCR/ABL, and TCC-Y/sr had the T315I mutation in the *BCR/ABL* gene.

— indicates not applicable.

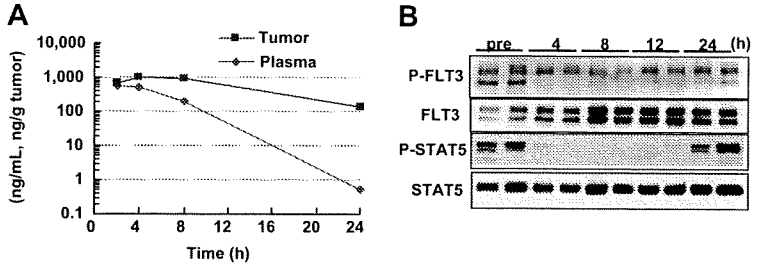

Figure 3. Pharmacokinetic and pharmacodynamic effects of KW-2449 in FLT3-activated leukemia. (A) MOLM-13 cells (10^7 cells/mouse) were subcutaneously inoculated into 2 SCID mice. Ten days after inoculation, KW-2449 at 20 mg/kg was orally administered twice every 12 hours. The concentrations of KW-2449 in plasma and tumor were sequentially analyzed by LC/MS/MS after the final administration of KW-2449. (B) The transition of FLT3 and STAT5 phosphorylation levels in tumor were analyzed by Western blotting. For analysis of FLT3 and its phosphorylated form (P-FLT3), the blots of immunoprecipitated FLT3 SDS-PAGE samples were analyzed by antiphospho-tyrosine (P-Tyr) antibody and anti-FLT3 antibody. For detection of STAT5 and its phosphorylated form (P-STAT5), total tumor lysate SDS-PAGE samples were analyzed by anti–P-STAT5 antibody and anti-STAT5 antibody as primary antibodies. Dephosphorylations of FLT3 and STAT5 in MOLM-13 were observed until 12 hours after the last administration. Results from 2 mice at each point are shown.

In vivo effects of KW-2449 on leukemia cells with FLT3 mutation

In vivo antileukemia activities of KW-2449 were evaluated using MOLM-13, FLT3-ITD AML, xenograft model. First, the concentrations of KW-2449 in both plasma and tumor after oral administration were sequentially examined in SCID mice bearing the subcutaneous MOLM-13 tumor. The tumor/plasma concentration ratio of KW-2449 tended to increase along with the time after administration and reached approximately 400, 24 hours after dosing (Figure 3A). The levels of P-FLT3 and P-STAT5 in the tumor were completely reduced from 4 to 12 hours after the administration of KW-2449 (Figure 3B). Although dephosphorylations of FLT3 and STAT5 were observed until 12 hours after administration, these returned to almost the basal level at 24 hours. These results suggested that the oral administration of KW-2449 at a twice daily schedule could be adequate for continuous inhibition of activated FLT3 in the mouse model.

In the MOLM-13 tumor xenograft model, oral administration of KW-2449 for 14 days showed a potent and significant antitumor effect in a dose-dependent manner (Figure 4A). KW-2449 treatment at 2.5 and 5.0 mg/kg twice a day showed growth inhibition of tumors with the ratio of tumor volume in the treated to control mice minimum values (T/C_{min}) of 0.57 and 0.29, respectively (Figure 4B). Furthermore, KW-2449 treatment at 10 mg/kg twice a day showed tumor regression with T/C_{min} of 0.010 and treatment at 20 mg/kg twice a day completely eradicated tumors in all mice (Figure 4C).

We next compared the effects of KW-2449 on mutant FLT3-expressing cells with a conventional antileukemic agent, AraC, using the syngeneic transplantation mouse model. Human FLT3/ITD-ires-GFP-expressing 32D (FLT3/ITD-GFP-32D) cells were intravenously inoculated into syngeneic C3H/Hej mice, and then KW-2449, AraC, or vehicle was administered to the mice 11 days after inoculation for 4 days (Figure 5A). At the seventh day after inoculation, mean FLT3 transcript levels in PB were 24.4 plus or minus 6.7, 11.8 plus or minus 5.7, and 42.0 plus or minus 21.7 copies/μg RNA in vehicle-, KW-2449- and AraC-treated mice, respectively. In all vehicle-treated mice, FLT3 transcript level increased, and the mean FLT3 transcript level in PB on day 13 was 5869.6 plus or minus 1640.1 copies/μg RNA. In contrast, KW-2449 treatment repressed the expansion of FLT3/ITD-GFP-32D cells as the decrease of FLT3 transcript levels was observed in all mice, and the mean FLT3 transcript level in PB was 3.25 plus or minus 2.29 copies/μg RNA on day 13. The increase in FLT3 transcripts level in all AraC-treated mice was lower than that in vehicle-treated mice, although the effect of AraC treatment was limited as the mean FLT3 transcript level in PB was 882.7 plus or minus 305.5 copies/μg RNA on day 13. These results demonstrated that the repressive effects by KW-2449 on the expansion of FLT3/ITD-GFP-32D cells were significantly stronger than those by AraC ($P = .026$ by the repeated-measures analysis of variance; Figure 5B). Flow cytometry analysis revealed that KW-2449 significantly eradicated FLT3/ITD-GFP-32D cells from BM (the mean percentages of FLT3/ITD-GFP-32D cells in BM after

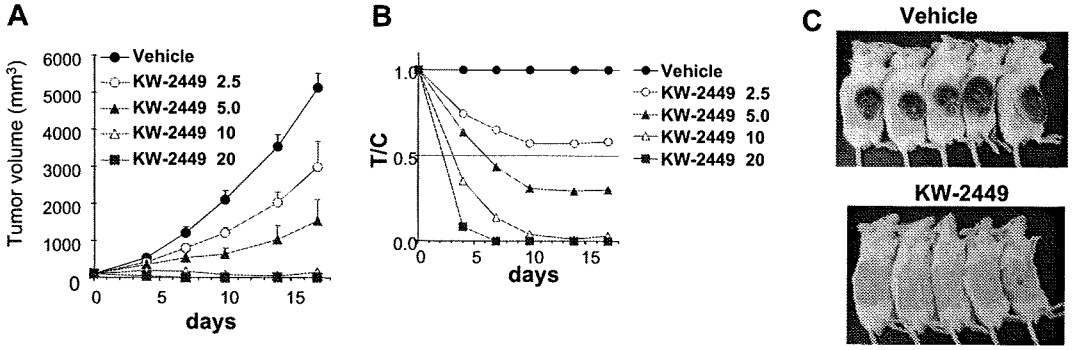

Figure 4. In vivo efficacy of xenotransplanted tumors with FLT3/ITD. (A-C) MOLM-13 cells (10^7 cells/mouse) were subcutaneously inoculated into SCID mice. Five days after inoculation, tumor volume was measured. The 25 mice with tumors ranging from 90 to 130 mm^3 were selected 5 days after inoculation and divided into 5 groups. Mice ($n = 5$ in each group) were orally administered with vehicle or KW-2449 (2.5, 5.0, 10, and 20 mg/kg) twice a day for 14 days. (A) Tumor volume was measured twice a week during the treatment. Mean tumor volume ± SD is shown. KW-2449 showed potent and significant antitumor effect in a dose-dependent manner. (B) Relative ratio of tumor volume (V) to initial tumor volume (V0) was represented (V/V0). Relative V/V0 ratio of a drug-treated group compared with a control group was represented as T/C. (C) KW-2449 treatment at 20 mg/kg twice a day showed complete regression and disappearance of tumors in all mice.

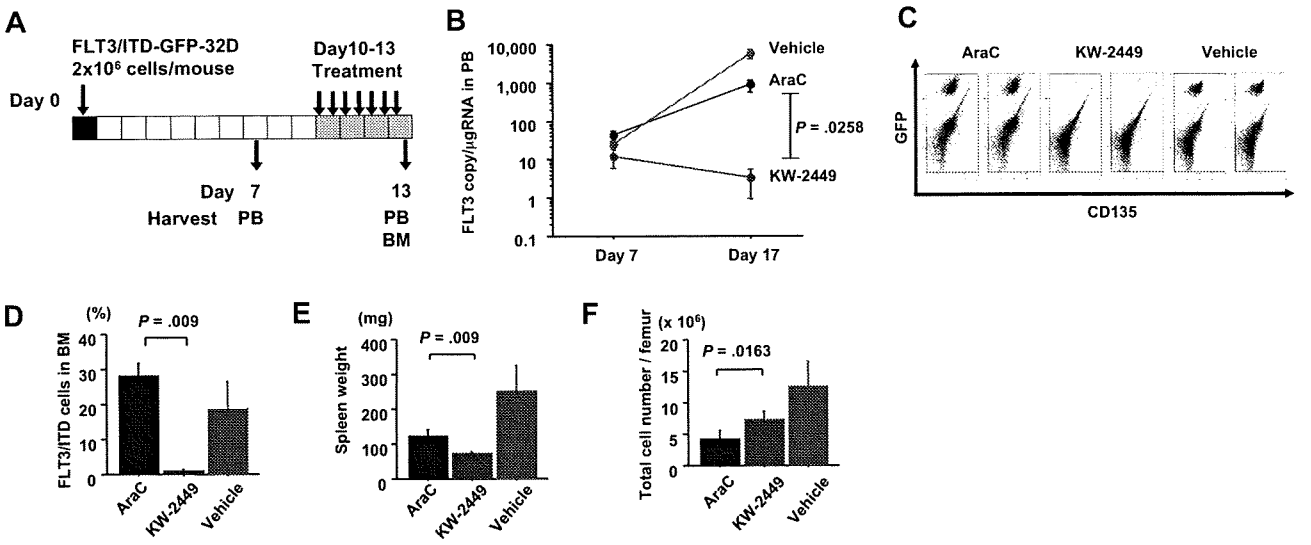

Figure 5. Inhibition effects on FLT3/ITD-GFP-32D cells in C3H/Hej-mice syngeneic transplantation model. (A) C3H/Hej mice were inoculated with 2×10^6 of FLT3/ITD-GFP-32D cells on day 0. From the 10th day after inoculation, mice were administrated with KW-2449 at 40 mg/kg (orally) twice a day, AraC at 150 mg/kg (intravenously) daily or vehicle for 4 days (n = 5 in each group). PB was collected from each mouse on day 7 and day 13. BM was collected on day 13. (B) Human FLT3 transcripts in PB were quantitated by a real-time fluorescence detection method. Mean transcript level ± SEM is shown. KW-2449 treatment significantly repressed the expansion of FLT3/ITD-GFP-32D cells compared with AraC treatment ($P = .026$ by the repeated-measures analysis of variance method). (C) The percentage of residual BM FLT3/ITD-GFP-32D cells in femur was compared among vehicle-, KW-2449-, and AraC-treated mice using flow cytometry. Representative results of flow cytometry are shown. (D) Mean percentages of residual FLT3/ITD-GFP-32D cells plus or minus SD in BM are shown. KW-2449 significantly eradicated FLT3/ITD-GFP-32D cells from BM compared with AraC treatment ($P = .009$ by the Mann-Whitney U test). (E) Mean spleen weight of each treated mouse ± SD is shown. The mean spleen weight of KW-2449-treated mice was significantly lighter than that of AraC-treated mice ($P = .009$ by the Mann-Whitney U test). (F) Mean total cell numbers in femur after the treatment ± SD are shown. The total number of nuclear cells in the BM of AraC-treated mice was significantly decreased compared with that of KW-2449–treated mice ($P = .016$ by the Mann-Whitney U test).

treatment were 30.0% ± 3.6% and 0.75% ± 0.75% in AraC- and KW-2449-treated mice, respectively; $P = .009$ by the Mann-Whitney U test; Figure 5C-D). Furthermore, the mean spleen weight of KW-2449-treated mice was significantly lighter than that of AraC-treated mice (71.4 ± 6.2 and 122.2 ± 20.4 mg, respectively; $P = .009$ by the Mann-Whitney U test; Figure 5E). Notably, the total number of nuclear cells in the BM of AraC-treated mice was significantly decreased compared with that of KW-2449-treated mice ([4.2 ± 1.3] × 10^6 and [7.3 ± 1.3] × 10^6 cells/femur, respectively; $P = .016$ by the Mann-Whitney U test; Figure 5F). In this model, we confirmed that KW-2449 could potently and selectively eradicate mutant FLT3-expressing leukemia cells both in PB and BM in contrast to the nonselective BM suppression of conventional cytotoxic agents such as AraC.

In vitro effects of KW-2449 on FLT3 wild-type leukemia

On the other hand, KW-2449 inhibited the growth of human ALL cell line RS4;11, which expresses unphosphorylated wt-FLT3, with the GI_{50} value of 0.23 μM (Table 2). Because KW-2449 shows potent Aurora A and Aurora B kinase inhibition, we evaluated whether the growth inhibitory effect on RS4;11 was induced by Aurora kinase inhibition. When the cell cycle was arrested in the M-phase by nocodazole, phosphorylated histone-H3 (P-HH3) was clearly observed in RS4;11, but it was decreased by the treatment with KW-2449 in a dose-dependent manner (Figure 6A). Cell cycle distribution analysis indicated that KW-2449 (0.60 μM) induced G_2/M arrest and apparent increase of sub-G_1 apoptotic cells after 24 hours and 48 hours of exposure, respectively (Figure 6B). Even at 0.30 μM, KW-2449 slightly decreased the population of S-phase cells from 49.0% to 40.6% after 72 hours (histogram data not shown). The increase of annexin V–positive (early apoptotic) cells was also observed at the GI_{50} value against RS4;11 cells (Figure 6C). These results suggested that KW-2449 has a growth inhibitory potency against leukemia cells even without activated FLT3 through the inhibition of Aurora kinase, although its potency was 5- to10-fold lower than that against those with activated FLT3 kinase.

Effects of KW-2449 on wt and T315I-mutated BCR/ABL-expressing leukemia cells

IM resistance is a critical issue to be resolved in the treatment of patients with BCR/ABL-positive leukemia. Because KW-2449 showed potency against both ABL and ABL-T315I kinases in the in vitro kinase assays, we evaluated its growth inhibitory effects on wt (K562 and TCC-Y) and T315I-mutated (TCC-Y/sr) BCR/ABL-expressing human leukemia cell lines. IM inhibited the growth of K562 and TCC-Y cells with GI_{50} values of 0.24 and 0.18 μM, respectively, whereas its GI_{50} value against TCC-Y/sr was 24 μM, which was approximately 100-fold higher than against K562 and TCC-Y cells. However, KW-2449 equally inhibited the growth of wt and T315I-mutated BCR/ABL-expressing leukemia cells: GI_{50} values were 0.27, 0.49, and 0.42 μM in K562, TCC-Y, and TCC-Y/sr cells, respectively (Table 2). In K562 cells, IM decreased the phosphorylation levels of BCR/ABL and STAT5 (Figure 7A), increased the number of the G_1 phase-arrested cells at 0.5 μM, and induced apoptosis, which was also shown by an increase of cleaved PARP (Figure 7A,D). On the other hand, KW-2449 induced G_2/M phase-arrested cells at 0.50 μM and increased the sub-G_1 and polyploidy cells at 1.0 μM (Figure 7D). These inductions of G_2/M arrest and polyploidy in K562 cells are presumed to be caused both by the Aurora A and Aurora B inhibitory profile of KW-2449. In TCC-Y cells, the IM treatment at 0.5 and 1.0 μM decreased the phosphorylation levels of BCR/ABL and STAT5, whereas it did not increase the apoptotic or the G_1 phase-arrested cells. In contrast, KW-2449 decreased the phosphorylation levels of BCR/ABL and STAT5 from 0.25 μM and induced the G_2/M-arrested cells at

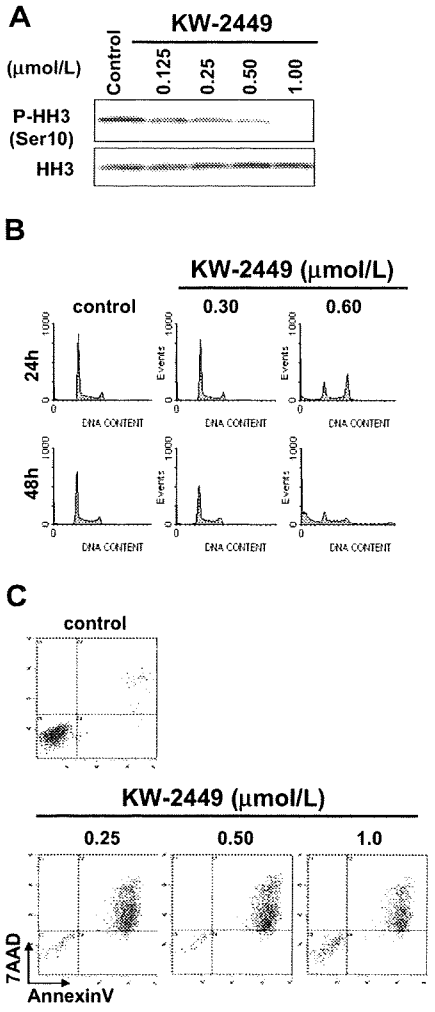

Figure 6. Effects of KW-2449 on human leukemia cells without FLT3 mutation. (A) RS4;11 cells, which express wild-type FLT3/ITD, were treated with KW-2449 at the indicated concentrations for 30 minutes. Total and phosphorylation levels of HH3 were analyzed by Western blotting. (B) RS4;11 cells were treated with various concentrations of KW-2449 for 48 hours, and cell-cycle distribution was analyzed. (C) RS4;11 cells were treated with various concentration of KW-2449 for 48 hours, and apoptosis induction was analyzed.

0.25 μM (data not shown), as well as apoptosis at 1.0 μM (Figure 7B,D). In TCC-Y/sr cells, IM did not affect the phosphorylation levels of BCR/ABL and STAT5 as well as apoptosis and the cell cycle, whereas KW-2449 decreased both phosphorylation levels from 0.25 and 0.5 μM, respectively. Furthermore, KW-2449 apparently induced apoptosis at 1.0 μM, which was shown by PARP cleavage and the sub-G_1 population (Figure 7C-D).

We next compared the effects of KW-2449 on human CML-BC cells harboring T315I mutation with IM, using the xenotransplantation mouse model. After confirming the engraftment of human CML-BC cells, NOD/SCID mice were administered with KW-2449, IM, or vehicle for 5 days. After the treatment, the BCR/ABL transcript levels in PB increased to 3.391 plus or minus 1.071 and 1.927 plus or minus 0.332 times as much as those before the treatment in the vehicle- and IM-treated mice, respectively. In contrast, KW-2449 significantly decreased BCR/ABL transcript levels as to 0.553 plus or minus 0.288 times as much as those before treatment compared with the vehicle- and IM-treated mice ($P = .001$ and $P = .003$ by the unpaired t test, respectively; Figure 7E). Furthermore, the immunohistochemical analysis showed that KW-2449 dramatically eradicated leukemia cells in BM (Figure 7F). In addition, KW-2449 treatment significantly prolonged the survival time of TCC-Y/sr-inoculated SCID mice (data not shown). These results collectively suggested that KW-2449 potently suppresses the growth both of wt- and T315I-mutated BCR/ABL-expressing leukemia cells by dual-inhibitory activities against BCR/ABL and Aurora kinases.

Discussion

Here we describe how KW-2449 potently and selectively inhibits the growth of leukemia cells harboring constitutively activated FLT3 kinase both in vitro and in vivo. As described previously, KW-2449 was selected from chemical libraries of Kyowa Hakko Kirin as a highly potent compound whose GI_{50} values against MOLM-13 and FLT3-D835Y-expressing 32D cells were less than 0.10 μM. In parallel, we evaluated the growth inhibitory activities against BCR/ABL-positive K562 cells and several hematologic malignant cell lines. As shown in this study, KW-2449 inhibited FLT3, ABL, and ABL-T315I kinases. In addition to these tyrosine kinases, which are involved in oncogenic addiction of several leukemia cells, KW-2449 has inhibitory effect on Aurora kinase, which is a key regulatory kinase in mitosis. Because KW-2449 potently inhibited the proliferation of various hematologic malignant cells, including wt-BCR/ABL– and T315I-mutated BCR/ABL-expressing cells, with GI_{50} values ranging from 0.014 to 0.65 μM, we evaluated which kinase was targeted in each malignant cell. To address this issue, we analyzed the phosphorylation status of possibly targeted kinases and the cell cycle distribution after KW-2449 treatment. In mutant FLT3-expressing leukemia cells, the reduction of P-FLT3 level was observed from less than 0.030 μM of KW-2449, which was consistent with its growth inhibitory and the G_1-arrest effects. In leukemia cells without FLT3 activation such as RS4;11, the sensitivity of KW-2449 was 5- to 10-fold lower than that in mutant FLT3-expressing leukemia cells. In these cells, KW-2449 induced the G_2/M arrest or polyploidy and apoptosis at approximately GI_{50} value (0.25 μM) via Aurora kinase inhibition, which was detected by the reduction of P-HH3. It has been reported that P-HH3 is the target molecule of Aurora B kinase, and the decrease of P-HH3 level was observed from 0.125 μM (Figure 6A), whereas G_2/M arrest, an indicator of Aurora kinase A inhibition, was clear at 0.60 μM of KW-2449. It suggested that both Aurora B and Aurora A kinase inhibition by KW-2449 contributes antileukemia effects in FLT3 wild-type. These results collectively suggested that KW-2449 potently suppressed the growth of leukemia cells immortalized by FLT3 activation via FLT3 inhibition alone at a lower concentration, whereas the growth suppression of FLT3-inactivated leukemia cells was induced by Aurora inhibition at a higher concentration. It has been reported that several kinase inhibitors, such as MK-0457 (VX-680), simultaneously suppress both FLT3 and Aurora kinases.[34] When we examined the effects of MK-0457 on mutant FLT3-expressing leukemia cells, it induced the G_2/M arrest at the GI_{50} values, indicating that its primary cellular target was Aurora kinase, but not FLT3 even in the constitutively FLT3-activated cells (data not shown). However, KW-2449 first inhibits FLT3 kinase with approximately 10-fold higher potency than Aurora kinase. Therefore, this characteristic mode of inhibitory action may be advantageous over the adverse events associated with the Aurora kinase inhibition.

The clinical efficacy of both PKC-412 and CEP-701 given as monotherapy was reportedly unimpressive despite their high

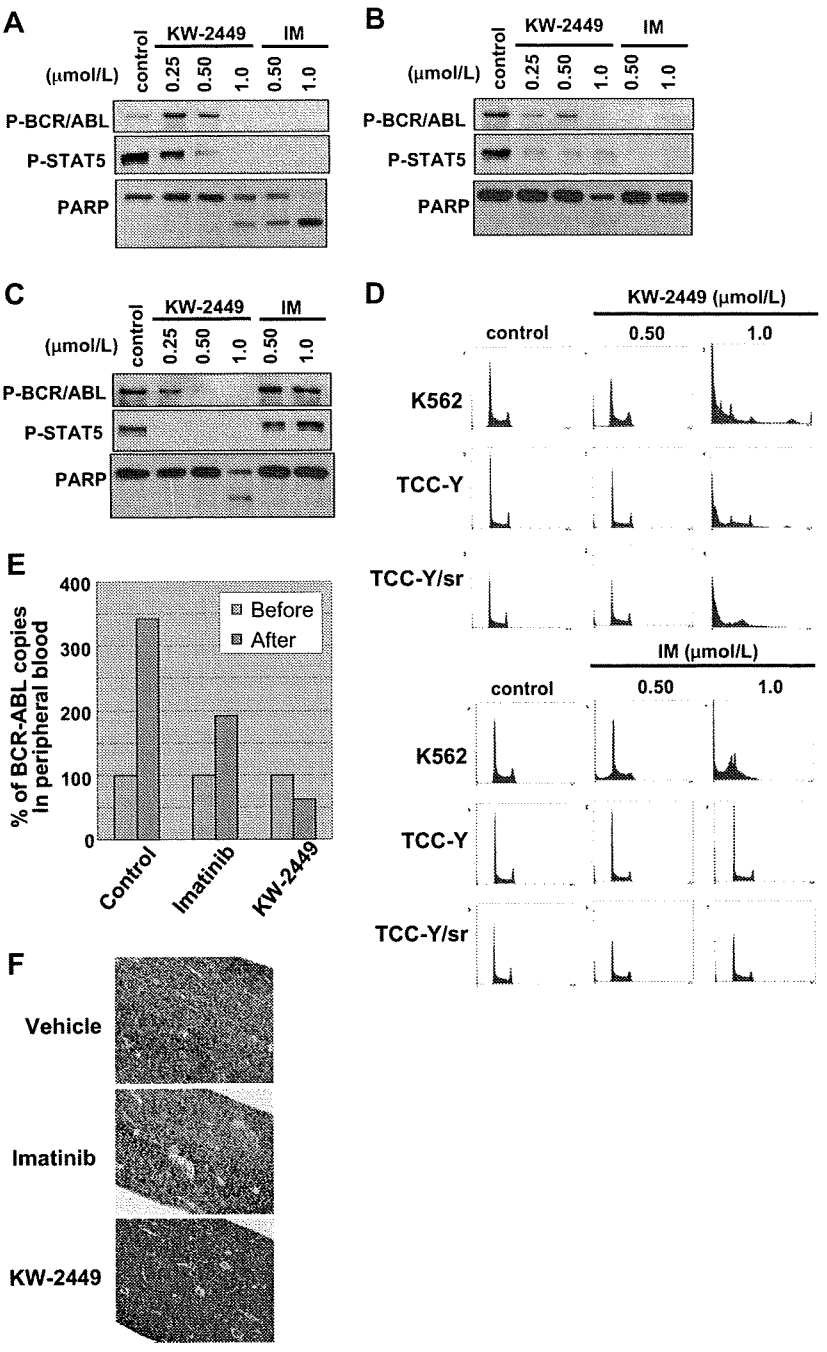

Figure 7. Inhibitory effects of KW-2449 on BCR/ABL-positive leukemia cells. We compared inhibitory effects on wt (K562 and TCC-Y) and T315I-mutated (TCC-Y/sr) BCR/ABL-expressing human leukemia cells between KW-2449 and imatinib (IM). (A) In K562 cells, KW-2449 and IM equally decreased the phosphorylation levels of BCR/ABL and STAT5 and increased cleaved PARP. (B) In TCC-Y cells, IM decreased the phosphorylation levels of BCR/ABL and STAT5, but did not increase cleaved PARP. In contrast, KW-2449 decreased the phosphorylation levels of BCR/ABL and STAT5 and increased cleaved PARP. (C) In TCC-Y/sr cells, IM did not affect the phosphorylation levels of BCR/ABL and STAT5, whereas KW-2449 decreased both phosphorylation levels and increased cleaved PARP. (D) DNA contents were also compared between KW-2449 and IM treatments. IM increased the number of the G_1-arrested cells only in K562 cells. However, KW-2449 induced the G_2/M-arrested cells in K562, TCC-Y, and TCC-Y/sr cells. (E) We compared the antileukemic efficacy in NOD/SCID mice xenotransplanted with human CML in blast crisis cells harboring the T315I mutation after IM treatment. The treatment effects on the leukemia cells in PB are shown by the after/before BCR/ABL transcript ratio. After the treatment, the BCR/ABL transcript levels in PB increased to 3.391 plus or minus 1.071 and 1.927 plus or minus 0.332 times as much as those before the treatment in the vehicle- and IM-treated mice, respectively. In contrast, KW-2449 significantly decreased BCR/ABL transcript levels as to 0.553 ± 0.288 times as much as those before the treatment compared with the vehicle- and IM-treated mice ($P = .001$ and $P = .003$ by the unpaired t test, respectively). (F) Residual leukemia cells in femora were evaluated by the immunohistochemical staining with human CD45. KW-2449 more potently eradicated leukemia cells in BM than IM.

potency in the in vitro studies and extensive exposure in humans. This was partly explained by their structural problem (both compounds are well known as tight binders to hAGP in human plasma) because they contain indolocarbazole motif and result in the significant reduction of their biologic activities in human bodies. In contrast, the growth inhibitory activity of KW-2449 was not attenuated by hAGP, indicating the advantage to keep the biologically active concentration in human plasma.

It is well known that IM that targets the adenosine triphosphate-binding site of the kinase domain of BCR/ABL, inducing remissions in patients with chronic-phase CML. However, whereas responses in the chronic phase were durable, remissions observed in blast crisis patients were typically short-lived, with relapse occurring within 6 months despite continued therapy. Thus, IM resistance is becoming an increasingly recognized problem for the treatment of patients with BCR/ABL-positive leukemia. Several IM-resistant mechanisms, such as acquired mutation in the *BCR/ABL* gene, overexpression of BCR/ABL, hAGP binding, and the emerging other kinase activations, have been reported.[35] To overcome the resistance, ABL kinase inhibitors in the second generation have been investigated, and some of them showed significant clinical response to IM-resistant or refractory patients, although the resistance of T315I-mutated BCR/ABL kinase remains to be resolved.[36] We therefore evaluated the efficacy of KW-2449 for leukemia cells with T315I-mutated BCR/ABL both in vitro and in vivo. KW-2449 at 0.25 μM showed the decrease of P-ABL and P-STAT5 in K562, TCC-Y, and TCC-Y/sr cells, whereas IM had little effect on these signaling molecules in T315I-mutated leukemia (Figure 7A). In addition to inhibitory activity of

KW-2449 to T315I-mutated BCR/ABL, Aurora kinase inhibition, which was indicated by cell-cycle distribution in TCC-Y/sr, could contribute to the release of IM resistance. On the other hand, whereas IM showed G_1 arrest and ABL inhibition in wt-BCR/ABL cells, it had limited activity both in cell cycle and cell signaling in T315I-mutated BCR/ABL cells. These data indicated that the inhibition of wt- and T315I-mutated BCR/ABL kinase by KW-2449 at lower concentrations showed limited effects on cell viability, whereas the additional inhibitory effects on Aurora kinase by KW-2449 at higher concentrations modulated the survival and proliferation of the IM-resistant leukemia cells. These multifunctional action mechanisms, as well as the order of potency against various kinases, which were involved in oncogenic addiction and drug-resistance, would contribute to overcome the IM resistance.

It has been reported that potent and selective Aurora kinase inhibitors show remarkable growth inhibition of a variety of cancer cells in vitro, although several severe adverse events such as hematopoietic toxicity have been observed in the early-phase clinical trials. However, our results suggest that the additive and/or simultaneous inhibition of Aurora kinase at a lower potency than mainly targeted kinases might contribute to increase the growth inhibitory effects on cancer cells without severe adverse effects.

In conclusion, targeted inhibition of FLT3 kinase with KW-2449 induced the potent growth inhibition of leukemia cells transformed by the constitutive activation of FLT3 kinase. KW-2449 also showed growth inhibitory effects against FLT3 leukemia by its Aurora kinase inhibition. In addition, simultaneous inhibition of T315I-mutated BCR/ABL and Aurora kinases by KW-2449 also induced the growth inhibition of IM-resistant leukemia cells. Currently, KW-2449 is being investigated in a phase 1/2 study in patients with relapsed or refractory AML (NCT00779480). The present results, nevertheless, provide an important insight into clinical investigations for the treatment of patients with BCR/ABL-positive leukemia acquiring the IM resistance, including the T315I-mutation.

Acknowledgments

The authors thank H. Kosugi for collecting clinical samples and S. Yamaji, E. Koshimura, M. Asano, and K. Higuchi for technical assistance.

This work was supported by the National Institute of Biomedical Innovation, Ministry of Health, Labor and Welfare, Ministry of Education, Culture, Sports, Science and Technology on the Scientific Research and the 21st Century COE Program Integrated Molecular Medicine for Neuronal and Neoplastic Disorders, Japan.

Authorship

Contribution: Y. Shiotsu designed experiments; screened chemical libraries; performed cell-based assay, Western blot, and animal studies; analyzed data; generated figures; and wrote the manuscript; H.K. designed experiments; performed Western blot, colony assay, animal studies, and quantitative real-time RT-PCR; analyzed data; generated figures; and wrote the manuscript; Y.I. collected clinical samples and performed Western blot and FCM; R.T. performed animal studies, quantitative real-time RT-PCR, and pathologic analysis; M.S. performed FCM analysis and Western blot; H.U. screened chemical libraries; K.I. performed Western blot and animal studies; Y. Mori performed colony assay; K.O. collected clinical samples and performed animal studies and quantitative real-time RT-PCR; Y. Minami performed cell cycle analysis; A.A. performed animal studies; H.M. analyzed the LC/MS/MS; T.A. and S.A. provided input into experiment design; Y.K. provided input into chemical synthesis; Y. Sato established imatinib-resistant cell lines; and T.N. designed experiments and wrote the manuscript.

Conflict-of-interest disclosure: Y. Shiotsu, M.S., H.U., K.I., H.M., T.A., Y.K., and S.A. are employed by Kyowa Hakko Kirin Co Ltd. H.K. has a consultancy with Kyowa Hakko Kirin Co Ltd.

Correspondence: Yukimasa Shiotsu, Fuji Research Park, Kyowa Hakko Kirin, 1188 Shimotogari, Nagaizumi-cho, Sunto-gun, Shizuoka 411-8731, Japan; e-mail: yukimasa.shiotsu@kyowa-kirin.co.jp.

References

1. Krause DS, Van Etten RA. Tyrosine kinases as targets for cancer therapy. *N Engl J Med.* 2005; 353:172-187.
2. Chalandon Y, Schwaller J. Targeting mutated protein tyrosine kinases and their signaling pathways in hematologic malignancies. *Haematologica.* 2005;90:949-968.
3. Druker BJ, Guilhot F, O'Brien SG, et al. Five-year follow-up of patients receiving imatinib for chronic myeloid leukemia. *N Engl J Med.* 2006;355:2408-2417.
4. Yanada M, Takeuchi J, Sugiura I, et al. High complete remission rate and promising outcome by combination of imatinib and chemotherapy for newly diagnosed BCR-ABL-positive acute lymphoblastic leukemia: a phase II study by the Japan Adult Leukemia Study Group. *J Clin Oncol.* 2006;24:460-466.
5. Stirewalt DL, Radich JP. The role of FLT3 in haematopoietic malignancies. *Nat Rev Cancer.* 2003;3:650-665.
6. Gilliland DG, Griffin JD. The roles of FLT3 in hematopoiesis and leukemia. *Blood.* 2002;100: 1532-1542.
7. Nakao M, Yokota S, Iwai T, et al. Internal tandem duplication of the flt3 gene found in acute myeloid leukemia. *Leukemia.* 1996;10:1911-1918.
8. Yamamoto Y, Kiyoi H, Nakano Y, et al. Activating mutation of D835 within the activation loop of FLT3 in human hematologic malignancies. *Blood.* 2001;97:2434-2439.
9. Kiyoi H, Yanada M, Ozekia K. Clinical significance of FLT3 in leukemia. *Int J Hematol.* 82:85-92.
10. Ozeki K, Kiyoi H, Hirose Y, et al. Biologic and clinical significance of the FLT3 transcript level in acute myeloid leukemia. *Blood.* 2004;103:1901-1908.
11. Gale RE, Hills R, Kottaridis PD, et al. No evidence that FLT3 status should be considered as an indicator for transplantation in acute myeloid leukemia (AML): an analysis of 1135 patients, excluding acute promyelocytic leukemia, from the UK MRC AML10 and 12 trials. *Blood.* 2005;106: 3658-3665.
12. Sternberg DW, Licht JD. Therapeutic intervention in leukemias that express the activated fms-like tyrosine kinase 3 (FLT3): opportunities and challenges. *Curr Opin Hematol.* 2005;12:7-13.
13. Stone RM, DeAngelo DJ, Klimek V, et al. Patients with acute myeloid leukemia and an activating mutation in FLT3 respond to a small-molecule FLT3 tyrosine kinase inhibitor, PKC412. *Blood.* 2005;105:54-60.
14. Fiedler W, Serve H, Döhner H, et al. A phase 1 study of SU11248 in the treatment of patients with refractory or resistant acute myeloid leukemia (AML) or not amenable to conventional therapy for the disease. *Blood.* 2005;105:986-993.
15. Knapper S, Burnett AK, Littlewood T, et al. A phase 2 trial of the FLT3 inhibitor lestaurtinib (CEP701) as first line treatment for older patients with acute myeloid leukemia not considered fit for intensive chemotherapy. *Blood.* 2006;108:3262-3270.
16. DeAngelo DJ, Stone RM, Heaney ML, et al. Phase 1 clinical results with tandutinib (MLN518), a novel FLT3 antagonist, in patients with acute myelogenous leukemia or high-risk myelodysplastic syndrome: safety, pharmacokinetics, and pharmacodynamics. *Blood.* 2006;108:3674-3681.
17. Knapper S. FLT3 inhibition in acute myeloid leukaemia. *Br J Haematol.* 2007;138:687-699.
18. Levis M, Pham R, Smith BD, Small D. In vitro studies of a FLT3 inhibitor combined with chemotherapy: sequence of administration is important to achieve synergistic cytotoxic effects. *Blood.* 2004;104:1145-1150.
19. Yee KW, Schittenhelm M, O'Farrell AM, et al. Synergistic effect of SU11248 with cytarabine or daunorubicin on FLT3 ITD-positive leukemic cells. *Blood.* 2004;104:4202-4209.
20. Kiyoi H, Naoe T. Biology, clinical relevance, and molecularly targeted therapy in acute leukemia